

Smoothing the Payoff for Efficient Computation of Option Pricing in Time-Stepping Setting

1 Introduction

1.1 The goal and outline of the project

The first goal of the project is to approximate $E[f(X(t))]$, using multi-index stochastic collocation(MISC) method, proposed in [11], where

- The payoff $f : \mathbb{R}^d \rightarrow \mathbb{R}$ has either jumps or kinks. Possible choices of f that we wanted to test are:
 - hockey-stick function, i.e., put or call payoff functions;
 - indicator functions (both relevant in finance (binary option,...) and in other applications of estimation of probabilities of certain events);
 - delta-functions for density estimation (and derivatives thereof for estimation of derivatives of the density).

More specifically, f should be the composition of one of the above with a smooth function. (For instance, the basket option payoff as a function of the log-prices of the underlying.)

- The process X is simulated via a time-stepping scheme. Possible choices that we wanted to test are
 - The one/multi dimensional discretized Black-Scholes(BS) process where we compare different ways to identify the location of the kink, such as:
 - * Exact location of the continuous problem
 - * Exact location of the discrete problem by root finding of a polynomial in y .
 - * Newton iteration.
 - A relative simple interest rate model or stochastic volatility model, for instance CIR or Heston models: In fact, the impact of the Brownian bridge will disappear in the limit, which may make the effect of the smoothing, but also of the errors in the kink location difficult to identify. For this reason, we suggest to study a more complicated 1-dimensional problem next. We suggest to use a CIR process. To avoid complications at the boundary, we suggest "nice" parameter choices, such that the discretized process is very unlikely to hit the boundary (Feller condition).

- The multi dimensional discretized Black-Scholes(BS) process: Here, we suggest to return to the Black-Scholes model, but in multi-dimensional case. In this case, linearizing the exponential, suggest that a good variable to use for smoothing might be the sum of the final values of the Brownian motion. In general, though, one should probably eventually identify the optimal direction(s) for smoothing via the duals algorithmic differentiation.

The desired outcome is a paper including

- Theoretical results including: i) an analiticity proof for the integrand in the time stepping setting, ii) a numerical analysis of the schemes involved, such as Newton iteration, etc.
- Applications that tests the examples above.

What has beed achieved so far:

1. Numerical outputs:

- **Example 1:** Tests for the basket option with the smoothing trick as in [2]: in that example we checked the performance of MISC without time stepping scheme and also compare the results with reference [2] (See Section 5.7). (Done).
- **Example 2:** The one dimensional binary option under discretized BS model (see Section 5.4). The results are promising (See Section 5.4) (Done).
- **Example 3:** The one dimensional call option under discretized BS model (see Section 5.5). The results are promising (See Section 5.5) (Done).
- **Example 4:** The multi dimensional basket call option under discretized BS model (see Section 5.2). (Under process).

2. Theoretical outputs:

- Heuristic proof of analiticity.

1.2 Literature review

Many option pricing problems require the computation of multivariate integrals. The dimension of these integrals is determined by the number of independent stochastic factors (e.g. the number of time steps in the time discretization or the number of assets under consideration). The high dimension of these integrals can be treated with dimension-adaptive quadrature methods to have the desired convergence behavior.

Unfortunately, in many cases, the integrand contains either kinks and jumps. In fact, an option is normally considered worthless if the value falls below a predetermined strike price. A kink (discontinuity in the gradients) is present when the payoff function is continuous, while a jump (discontinuity in the function) exists when the payoff coreesponds to a binary or other digital options. The existence of kinks or jumps in the integrand heavily degrades the performance of quadrature formulas. In this work, we are interested in solving this problem by using adaptive sparse grids (SG) methods coupled with suitable transformations. The main idea is to find lines or areas of discontinuity and to employ suitable transformations of the integration domain. Then by a pre-integration (smoothing) step with respect to the dimension containing the kink/jump, we

end up with integrating only over the smooth parts of the integrand and the fast convergence of the sparse grid method can be regained.

One can ignore the kinks and jumps, and apply directly a method for integration over \mathbb{R}^d . Despite the significant progress in SG methods [3] for high dimensional integration of smooth integrands, few works have been done to deal with cases involving integrands with kinks or jumps due to the decreasing performance of SG methods in the presence of kinks and jumps.

Some works [8, 2, 9, 10, 16] addressed similar kind of problems, characterized by the presence of kinks and jumps, but with much more emphasis on Quasi Monte Carlo (QMC). In [8, 9, 10], an analysis of the performance of Quasi Monte Carlo (QMC) and SG methods has been conducted, in the presence of kinks and jumps. In [8, 9], the authors studied the terms of the ANOVA decomposition of functions with kinks defined on d -dimensional Euclidean space \mathbb{R}^d , and showed that under some assumptions all but the the highest order ANOVA term of the 2^d ANOVA terms can be smooth for the case of an arithmetic Asian option with the Brownian bridge construction. Furthermore, [10] extended the work in [8, 9] from kinks to jumps for the case of an arithmetic average digital Asian option with the principal component analysis (PCA). The main findings in [8, 9] was obtained for an integrand of the form $f(\mathbf{x}) = \max(\phi(\mathbf{x}), 0)$ with ϕ being smooth. In fact, by assuming i) the d -dimensional function ϕ has a positive partial derivative with respect to x_j for some $j \in \{1, \dots, d\}$, ii) certain growth conditions at infinity are satisfied, the authors showed that the ANOVA terms of f that do not depend on the variable x_j are smooth. We note that [8, 9, 10] focus more on theoretical aspects of applying QMC in such a setting. On the other hand, we focus more on specific practical problems, where we add the adaptivity paradigm to the picture.

A recent work [16] addresses similar kind of problems using QMC. Being very much related to [2], the authors i) assume that the conditional expectation can be computed explicitly, by imposing very strong assumptions. ii) Secondly, they use PCA on the gradients to reduce the effective dimension. In our work, we do not make such assumptions, which is why we need numerical methods, more precisely root finding and the quadrature in the first direction.

2 Problem formulation and Setting

In the context of option pricing, we aim at approximating the option price, $E[g(\mathbf{X}(t))]$, where $g : \mathbb{R}^d \rightarrow \mathbb{R}$ is the payoff function and where the process of the asset prices $\mathbf{X} \in \mathbb{R}^d$ solves

$$(1) \quad \mathbf{X}(t) = \mathbf{X}(0) + \int_0^t a(s, \mathbf{X}(s))ds + \sum_{\ell=1}^{\ell_0} \int_0^t b^\ell(s, \mathbf{X}(s))dW^\ell(s)$$

Let us denote by $\Phi : (\mathbf{z}_1, \dots, \mathbf{z}_N) \rightarrow \mathbf{X}_T$, the mapping consisting of the time-stepping scheme, where $\{\mathbf{z}_i\}_{i=1}^N$ are independent d -dimensional Gaussian random vectors, and N is the number of time steps. Without loss of Generality, we assume that Φ may include pre-processing transformations to reduce the effective dimension. We also assume that $d = 1$ and the extension to higher dimension is trivial.

In this setting, we are interetsed in the basic problem of approximating

$$(2) \quad E[g(\mathbf{X}(t))] = I_N(g \circ \Phi) := \int_{\mathbb{R}^N} g \circ \Phi(\mathbf{z})d\mathbf{z} = \int_{-\infty}^{\infty} \dots \int_{-\infty}^{\infty} g \circ \Phi(z_1, \dots, z_N)\rho_d(\mathbf{z})dz_1, \dots, dz_N,$$

with

$$(3) \quad \rho_N(\mathbf{z}) = \frac{1}{(2\pi)^{N/2}} e^{-\frac{1}{2}\mathbf{z}^T \mathbf{z}}.$$

where ρ is a continuous and strictly positive probability density function on \mathbb{R} and g is a real-valued function integrable with respect to ρ_N .

In this context, we work mainly with two possible structures of payoff function g . In fact, for the cases of call/put options, the payoff g has a kink and will be of the form

$$(4) \quad g(\mathbf{x}) = \max(\phi(\mathbf{x}), 0).$$

One can also encounter jumps in the payoff when working with binary digital options. In this case, g is given by

$$(5) \quad g(\mathbf{x}) = \mathbf{1}_{(\phi(\mathbf{x}) \geq 0)}.$$

We introduce the notation $\mathbf{x} = (x_j, \mathbf{x}_{-j})$, where \mathbf{x}_{-j} denotes the vector of length $d-1$ denoting all the variables other than x_j . Then, if we assume for some $j \in \{1, \dots, d\}$

$$(6) \quad \frac{\partial \phi}{\partial x_j}(\mathbf{x}) > 0, \forall \mathbf{x} \in \mathbb{R}^d \quad \textbf{(Monotonicity condition)}$$

$$(7) \quad \lim_{x \rightarrow +\infty} \phi(\mathbf{x}) = \lim_{x \rightarrow +\infty} \phi(x_j, \mathbf{x}_{-j}) = +\infty, \text{ or } \frac{\partial^2 \phi}{\partial x_j^2}(\mathbf{x}) \quad \textbf{(Growth condition)},$$

then, using Fubini's theorem, we can rewrite (2) as

$$(8) \quad \begin{aligned} I_N(g \circ \Phi) &= \int_{\mathbb{R}^{d-1}} \left(\int_{-\infty}^{\infty} g \circ \Phi(z_j, \mathbf{z}_{-j}) \rho(z_j) dz_j \right) \rho_{z-1}(\mathbf{z}_{-j}) d\mathbf{z}_{-j}, \\ &= \mathbb{E} [E[g \circ \Phi(z_j, \mathbf{z}_{-j}) \mid z_j]] \end{aligned}$$

where we evaluate the inner integral for each \mathbf{z}_{-j} and which results in a smooth integrand for the outer $(N-1)$ -dimensional integral.

We note that conditions ((6) and (7)) imply that for each \mathbf{z}_{-j} , the function $\phi \circ \Phi(z_j, \mathbf{z}_{-j})$ either has a simple root z_j or is positive for all $z_j \in \mathbb{R}$.

We generally do not have a closed form for the inside integral in (8). Therefore, the pre-integration (conditional sampling) step should be performed numerically.

3 Details of our approach

In the following, we describe our approach which basically can be seen as a two stage method. In the first step, we use root finding procedure to get the inner integral in (8), then in a second stage we employ adaptive quadrature, multi-index stochastic collocation (MISC), to compute the obtained smooth integrand.

3.1 The one dimensional case

For illustration purposes, let us focus on the one dimensional case, where under the risk-neutral measure, the undelying asset follows the geometric Brownian motion (GBM)

$$(9) \quad dX_t = rX_t dt + \sigma X_t dB_t,$$

where r is the risk-free rate, σ is the volatility and B_t is the standard Brownian motion. The analytical solution to (9) is

$$(10) \quad X_t = X_0 \exp((r - \sigma^2)t + \sigma B_t).$$

The Brownian motion B_t can be constructed either sequentially using a standard random walk construction or hierarchically using Brownian bridge (Bb) construction. To make an effective use of MISC, which profits from anisotropy, we use the Bb construction since it produces dimensions with different importance for MISC (creates anisotropy), contrary to random walk procedure for which all the dimension of the stochastic space have equal importance (isotropic). We explain the Bb construction in Section 3.4.1.

Let us denote by $\psi : (z_1, \dots, z_N) \rightarrow (B_1, \dots, B_N)$ the mapping of Bb construction and by $\Phi : (B_1, \dots, B_N) \rightarrow X_T$, the mapping consisting of the time-stepping scheme. Then, we can express the option price as

$$(11) \quad \begin{aligned} \mathbb{E}[g(X(T))] &= \mathbb{E}[g(\Phi \circ \psi)(z_1, \dots, z_N)] \\ &= \int_{-\infty}^{\infty} \dots \int_{-\infty}^{\infty} G(z_1, \dots, z_N) \rho_N(\mathbf{z}) dz_1, \dots, dz_N, \end{aligned}$$

where $G = g \circ \Phi \circ \psi$ and

$$(12) \quad \rho_N(\mathbf{z}) = \frac{1}{(2\pi)^{N/2}} e^{-\frac{1}{2}\mathbf{z}^T \mathbf{z}}.$$

Now, we can easily apply the procedure of pre-integration of section 2, where we can assume that the payoff function g can be either the maximum or indicator function and $\phi = \Phi \circ \psi$. The remaining ingredient is to determine with respect to which variable z_j we will integrate.

Claiming that pre-integrating with respect to z_1 is the optimal option then from (11), we have

$$(13) \quad \begin{aligned} \mathbb{E}[g(X(T))] &= \int_{-\infty}^{\infty} \dots \int_{-\infty}^{\infty} G(z_1, \dots, z_N) \rho_N(\mathbf{z}) dz_1, \dots, dz_N \\ &= \int_{\mathbb{R}^{N-1}} \left(\int_{-\infty}^{\infty} G(z_1, \mathbf{z}_{-1}) \rho(z_1) dz_1 \right) \rho_{N-1}(\mathbf{z}_{-1}) d\mathbf{z}_{-1} \\ &= \int_{\mathbb{R}^{N-1}} h(\mathbf{z}_{-1}) \rho_{N-1}(\mathbf{z}_{-1}) d\mathbf{z}_{-1}, \\ &= \mathbb{E}[h(\mathbf{z}_{-1})] \end{aligned}$$

where $h(\mathbf{z}_{-1}) = \int_{-\infty}^{\infty} G(z_1, \mathbf{z}_{-1}) \rho(z_1) dz_1 = E[G(z_1, \dots, z_N) \mid z_1]$.

Since g can have a kink or jump. Computing $h(\mathbf{z}_{-1})$ in the pre-integration step should be carried carefully to not deteriorate the smoothness of h . This can be done by applying a root finding procedure and then computing the uni-variate integral by summing the terms coming from integrating in each region where g is smooth. In Sections (3.6,3.7), we explain those points.

Once we perform stage 1 procedure, we use multi-index stochastic collocation (MISC) procedure, suggested in [11], to compute the expectation $E[h(\mathbf{z}_{-1})]$. We describe the general strategy for the multi-index construction in Section 3.3.

We have a natural error decomposition for the total error of computing the expectation in (13), namely, \mathcal{E}

$$(14) \quad \mathcal{E} \leq \mathcal{E}_Q(TOL_{\text{MISC}}, N) + \mathcal{E}_B(N),$$

where \mathcal{E}_Q is the quadrature error, function of MISC tolerance TOL_{MISC} and N (the number of time steps) and \mathcal{E}_B is the bias, function of N (the number of time steps) or $\Delta_t = \frac{T}{N}$ (size of the time grid).

3.2 Extension to the high dimensional case

In the high dimensional case, we denote by $(z_1^{(i)}, \dots, z_N^{(i)})$ the N Gaussian independent rdvs that will be used to construct the path of the i -th asset $X^{(i)}$, where $1 \leq i \leq d$ (d denotes the number of underlyings considered in the basket). We keep the same notations by denoting $\psi : (z_1^{(i)}, \dots, z_N^{(i)}) \rightarrow (B_1, \dots, B_N)$ the mapping of Bb construction and by $\Phi : (B_1^{(i)}, \dots, B_N^{(i)}) \rightarrow X_T^{(i)}$, the mapping consisting of the time-stepping scheme. Then, we can express the option price as

$$(15) \quad \begin{aligned} E[g(\mathbf{X}(T))] &= E \left[g(\Phi \circ \psi)(z_1^{(1)}, \dots, z_N^{(1)}, \dots, z_1^{(d)}, \dots, z_N^{(d)}) \right] \\ &= \int_{\mathbb{R}^{d \times N}} G(z_1^{(1)}, \dots, z_N^{(1)}, \dots, z_1^{(d)}, \dots, z_N^{(d)}) \rho_{d \times N}(\mathbf{z}) dz_1^{(1)} \dots dz_N^{(1)} \dots dz_1^{(d)} \dots dz_N^{(d)}, \end{aligned}$$

where $G = g \circ \Phi \circ \psi$ and

$$(16) \quad \rho_{d \times N}(\mathbf{z}) = \frac{1}{(2\pi)^{d \times N/2}} e^{-\frac{1}{2} \mathbf{z}^T \mathbf{z}}.$$

Now, performing the pre-integrating step with respect to the coarse rdvs $(z_1^{(1)}, \dots, z_1^{(d)})$, results in

$$(17) \quad \begin{aligned} E[g(\mathbf{X}(T))] &= \int_{\mathbb{R}^{d \times N}} G(z_1^{(1)}, \dots, z_N^{(1)}, \dots, z_1^{(d)}, \dots, z_N^{(d)}) \rho_{d \times N}(\mathbf{z}) dz_1^{(1)} \dots dz_N^{(1)} \dots dz_1^{(d)} \dots dz_N^{(d)} \\ &= \int_{\mathbb{R}^{d \times (N-1)}} \left(\int_{\mathbb{R}^d} G(z_1^{(1)}, \mathbf{z}_{-1}^{(1)}, \dots, z_1^{(d)}, \mathbf{z}_{-1}^{(d)}) \rho_d(z_1^{(1)}, \dots, z_1^{(d)}) dz_1^{(1)} \dots dz_1^{(d)} \right) \rho_{d \times (N-1)}(\mathbf{z}_{-1}^{(1)}, \dots, \mathbf{z}_{-1}^{(d)}) d\mathbf{z}_{-1}^{(1)} \dots d\mathbf{z}_{-1}^{(d)} \\ &= \int_{\mathbb{R}^{d \times (N-1)}} h(\mathbf{z}_{-1}^{(1)}, \dots, \mathbf{z}_{-1}^{(d)}) \rho_{d \times (N-1)}(\mathbf{z}_{-1}^{(1)}, \dots, \mathbf{z}_{-1}^{(d)}) d\mathbf{z}_{-1}^{(1)} \dots d\mathbf{z}_{-1}^{(d)}, \\ &= E \left[h(\mathbf{z}_{-1}^{(1)}, \dots, \mathbf{z}_{-1}^{(d)}) \right] \end{aligned}$$

where $h(\mathbf{z}_{-1}^{(1)}, \dots, \mathbf{z}_{-1}^{(d)}) = \int_{\mathbb{R}^d} G(z_1^{(1)}, \mathbf{z}_{-1}^{(1)}, \dots, z_1^{(d)}, \mathbf{z}_{-1}^{(d)}) \rho_d(z_1^{(1)}, \dots, z_1^{(d)}) dz_1^{(1)} \dots dz_1^{(d)}$.

3.3 The MISC solver

Assume we want to solve the problem of approximating the expected value of $E[f(Y)]$ on a tensorization of quadrature formulae over the stochastic domain, Γ . We also assume that $f(y)$ is a continuous function (analytic) over Γ .

To introduce simplified notations, we start with the one-dimension case. Let us define $\beta \leq 1$ be an integer positive value referred to as a "stochastic discretization level", and $m : \mathbb{N} \rightarrow \mathbb{N}$ be a strictly increasing function with $m(0) = 0$ and $m(1) = 1$, that we call a "level-to-nodes function". At level β , we consider a set of $m(\beta)$ distinct quadrature points in $(-\infty, \infty)$, $\mathcal{H}^{m(\beta)} = \{y_\beta^1, y_\beta^2, \dots, y_\beta^{m(\beta)}\} \subset [-\infty, \infty]$, and a set of quadrature weights, $\omega^{m(\beta)} = \{\omega_\beta^1, \omega_\beta^2, \dots, \omega_\beta^{m(\beta)}\}$. We also let $C^0((-\infty, \infty))$ be the set of real-valued continuous functions over $(-\infty, \infty)$. We then define the quadrature operator as

$$(18) \quad Q(m(\beta)) : C^0((-\infty, \infty)) \rightarrow \mathbb{R}, \quad Q(m(\beta))[f] = \sum_{j=1}^{m(\beta)} f(y_\beta^j) \omega_\beta^j.$$

In our case, and following (17), we have a multi-variate integration problem and we have, given the previous notations, $f := h$, $\mathbf{Y} = (\mathbf{z}_{-1}^{(1)}, \dots, \mathbf{z}_{-1}^{(d)})$, and Γ is finite dimensional and given by a $d(N-1)$ tensor product of intervals. Therefore, we define, for any multi-index β

$$Q^{m(\beta)} : \Gamma \rightarrow \mathbb{R}, \quad Q^{m(\beta)} = \bigotimes_{n=1}^{d(N-1)} Q^{m(\beta_n)}$$

where the n -th quadrature operator is understood to act only on the n -th variable of f . Practically, we obtain the value of $Q^{m(\beta)}[f]$ by considering the tensor grid $\mathcal{T}^{m(\beta)} = \times_{n=1}^{d(N-1)} \mathcal{H}^{m(\beta_n)}$ with cardinality $\#\mathcal{T}^{m(\beta)} = \prod_{n=1}^{d(N-1)} m(\beta_n)$ and computing

$$Q^{\mathcal{T}^{m(\beta)}}[f] = \sum_{j=1}^{\#\mathcal{T}^{m(\beta)}} f(\hat{y}_j) \bar{\omega}_j$$

where $\hat{y}_j \in \mathcal{T}^{m(\beta)}$ and $\bar{\omega}_j$ are products of weights of the univariate quadrature rules.

Remark 3.1. We note that the quadrature points are chosen to optimize the convergence properties of the quadrature error. For instance, in our context, since we are dealing with Gaussian densities, using Gauss-Hermite quadrature points is the appropriate choice.

A direct approximation $E[f[\mathbf{Y}]] \approx Q^{m(\beta)}[f]$ is not an appropriate option due to the well-known "curse of dimensionality" effect. We use MISC as it was suggested in [11]. MISC is a hierarchical adaptive sparse grids quadrature strategy that uses stochastic discretizations and classic sparsification approach to obtain an effective approximation scheme for $E[f]$.

For the sake of concreteness, in our setting from (17), we are left with a $d(N-1)$ -dimensional Gaussian random inputs, which are chosen independently, resulting in $d(N-1)$ numerical parameters for MISC, which we use as the basis of the multi-index construction. Let $l \in \{1, \dots, d(N-1)\}$ and set

$$(19) \quad p_l := z_{i1+1}, \quad 1 \leq i \leq d, \quad (i-1)(N-1) + 1 \leq l \leq i(N-1).$$

For a multi-index $\ell = (l_i)_{i=1}^{d(N-1)} \in \mathbb{N}^{d(N-1)}$, we denote by $Q_N^\ell := Q^{N,m(\ell)}(p_\ell)$ the result of a discretized integral, using N time steps, with parameters $p_\ell := (p_{l_i})_{i=1}^{d(N-1)}$, and with a number of quadrature points $m(l_i)$ in the dimension p_{l_i} . We further define the set of differences ΔQ_N^ℓ as follows: for a single index $1 \leq i \leq d(N-1)$, let

$$(20) \quad \Delta_i Q_N^\ell := \begin{cases} Q_N^\ell - Q_N^{\ell'} & \text{with } \ell' = \ell - e_i, \text{ if } \ell_i > 0 \\ Q_N^\ell & \text{otherwise} \end{cases}$$

where e_i denotes the i th $d(N-1)$ -dimensional unit vector. Then, ΔQ_N^ℓ is defined as

$$(21) \quad \Delta Q_N^\ell := \left(\prod_{i=1}^{d(N-1)} \Delta_i \right) Q_N^\ell.$$

We have the telescoping property

$$(22) \quad Q_N^\infty = \sum_{l_1=0}^{\infty} \cdots \sum_{l_{d(N-1)}=0}^{\infty} \Delta Q_N^{(l_1, \dots, l_{d(N-1)})} = \sum_{\ell \in \mathbb{N}^{d(N-1)}} \Delta Q_N^\ell,$$

provided that $l_1 \rightarrow \infty, \dots, l_{d(N-1)} \rightarrow \infty$, where Q_N^∞ is the biased option price, computed with N time steps.

As stated before, our goal is to approximate, Q_N^∞ , then the actual MISC estimator computed using a given a set of multi-indices $\mathcal{I} \subset \mathbb{N}^{d(N-1)}$, is given by

$$Q_N^{\mathcal{I}} := \sum_{\ell \in \mathcal{I}} \Delta Q_N^\ell.$$

The quadrature error in this case is given by

$$(23) \quad \mathcal{E}_Q(TOL_{\text{MISC}}, N) = |Q_N^\infty - Q_N^{\mathcal{I}}| \leq \sum_{\ell \in \mathbb{N}^{d(N-1)} \setminus \mathcal{I}} |\Delta Q_N^\ell|.$$

If we denote the computational work at level $\ell = (l_1, \dots, l_{d(N-1)})$, for adding an increment ΔQ_N^ℓ in the telescoping sum, by \mathcal{W}_N^ℓ , then the construction of the optimal \mathcal{I} will be done by profit thresholding, i.e., for a certain threshold value T , we add a multi-index ℓ to \mathcal{I} provided that

$$\log \left(\frac{|\Delta Q_N^\ell|}{\mathcal{W}_N^\ell} \right) \leq T.$$

3.4 Path generation methods (PGM)

In the literature of adaptive sparse grids and QMC, several hierarchical path generation methods (PGMs) or transformation methods have been proposed to reduce the effective dimension. Among these transformations, we cite the Brownian bridge (Bb) construction [14, 4, 13, 12], the principal component analysis (PCA) [1] and the linear transformation (LT) [?], etc ...

Assume that one wants to compute $E[g(B)]$, where B is a Brownian motion with index set $[0, T]$. In most applications this can be reasonably approximated by $E\left[\tilde{g}\left(B_{\frac{T}{N}}, \dots, B_{\frac{T}{N}}\right)\right]$, where \tilde{g} is a function of the set of discrete Brownian paths.

There are three classical methods for sampling from $(B_{\frac{T}{N}}, \dots, B_{\frac{TN}{N}})$ given a standard normal vector Z , namely the forward method, the Brownian bridge (Bb) construction and the principal component analysis (PCA) construction. All of these constructions may be written in the form $(B_{\frac{T}{N}}, \dots, B_{\frac{TN}{N}}) = AZ$, where A is an $N \times N$ real matrix with

$$AA^T = \Sigma := \left(\frac{T}{N} \min(j, k) \right)_{j,k=1}^N = \frac{T}{N} \begin{bmatrix} 1 & 1 & 1 & \dots & 1 \\ 1 & 2 & 2 & \dots & 2 \\ 1 & 2 & 3 & \dots & 3 \\ \vdots & \vdots & \vdots & \ddots & \vdots \\ 1 & 2 & 3 & \dots & N \end{bmatrix}.$$

For instance, the matrix A corresponding to the forward method is given by

$$A^F = \sqrt{\frac{T}{N}} \begin{bmatrix} 1 & 0 & \dots & 0 \\ 1 & 1 & \dots & 0 \\ \vdots & \vdots & \ddots & \vdots \\ 1 & 1 & \dots & 1 \end{bmatrix}.$$

In the case of Bb construction, details about the construction are given in Section 3.4.1, and the corresponding matrix A , For $N = 8$ is given by

$$A^{\text{Bb}} = \sqrt{T} \begin{bmatrix} \frac{1}{8} & \frac{1}{8} & \frac{\sqrt{2}}{8} & 0 & \frac{2}{8} & 0 & 0 & 0 \\ \frac{1}{8} & \frac{1}{8} & \frac{\sqrt{2}}{8} & 0 & \frac{2}{8} & 0 & 0 & 0 \\ \frac{1}{8} & \frac{1}{8} & \frac{\sqrt{2}}{8} & 0 & \frac{2}{8} & 0 & 0 & 0 \\ \frac{1}{8} & \frac{1}{8} & \frac{\sqrt{2}}{8} & 0 & \frac{2}{8} & 0 & 0 & 0 \\ \frac{1}{8} & \frac{1}{8} & \frac{\sqrt{2}}{8} & 0 & \frac{2}{8} & 0 & 0 & 0 \\ \frac{1}{8} & \frac{1}{8} & \frac{\sqrt{2}}{8} & 0 & \frac{2}{8} & 0 & 0 & 0 \\ \frac{1}{8} & \frac{1}{8} & \frac{\sqrt{2}}{8} & 0 & \frac{2}{8} & 0 & 0 & 0 \\ 1 & 0 & 0 & 0 & 0 & 0 & 0 & 0 \end{bmatrix}.$$

When doing PCA construction [1], we have $A^{\text{PCA}} = VD$, where $\Sigma = VD^2V^T$ is the singular value decomposition of Σ .

3.4.1 Brownian bridge (Bb) construction

In our context, sampling the Brownian motion can be constructed either sequentially using a standard random walk construction or hierarchically using other hierarchical PGM as listed above. For our purposes, to make an effective use of MISC, which profits from anisotropy, we use the Bb construction since it produces dimensions with different importance for MISC (creates anisotropy), contrary to random walk procedure for which all the dimension of the stochastic space have equal importance (isotropic). This pre-transformation reduces the effective dimension dimension of the problem and as a consequence accelerates the MISC procedure by reducing the computational cost.

Let us denote $\{t_i\}_{i=0}^N$ the grid of time steps, then the Bb construction [7] consists of the following: given a past value B_{t_i} and a future value B_{t_k} , the value B_{t_j} (with $t_i < t_j < t_k$) can be generated according to the formula:

$$(24) \quad B_{t_j} = (1 - \rho)B_{t_i} + \rho B_{t_k} + \sqrt{\rho(1 - \rho)(k - i)\Delta t}z, \quad z \sim \mathcal{N}(0, 1),$$

where $\rho = \frac{j-i}{k-i}$. In particular, if N is a power of 2, then given $B_0 = 0$, Bb generates the Brownian motion at times $T, T/2, T/4, 3T/4, \dots$ according

$$\begin{aligned}
B_T &= \sqrt{T}z_1 \\
B_{T/2} &= \frac{1}{2}(B_0 + B_T) + \sqrt{T/4}z_2 = \frac{\sqrt{T}}{2}z_1 + \frac{\sqrt{T}}{2}z_2 \\
B_{T/4} &= \frac{1}{2}(B_0 + B_{T/2}) + \sqrt{T/8}z_3 = \frac{\sqrt{T}}{4}z_1 + \frac{\sqrt{T}}{4}z_2 + \sqrt{T/8}z_3 \\
&\vdots
\end{aligned}
\tag{25}$$

where $\{z_j\}_{j=1}^N$ are independent standard normal variables.

Describing construction 25: we first generate the final value B_T , then sample $B_{T/2}$ conditional on the values of B_T and B_0 , and proceed by progressively filling in intermediate values. Bb uses the first several coordinates of the low-discrepancy points to determine the general shape of the Brownian path, and the last few coordinates influence only the fine detail of the path. Therefore, the most important values that determine the large scale structure of Brownian motion are the first components of $\mathbf{z} = (z_1, \dots, z_N)$.

3.5 Richardson extrapolation

Another pre-transformation that we coupled with MISC is Richardson extrapolation [15]. In fact, applying level ℓ of Richardson extrapolation reduces dramatically the bias and as a consequence reduces the needed number of time steps N used in the coarsest level to achieve a certain error tolerance. This means basically that Richardson extrapolation reduces directly the total dimension of the integration problem for achieving some error tolerance.

We recall that the Euler (often) scheme has weak order 1 so that

$$\left| \mathbb{E} \left[f(\hat{X}_T^h) \right] - \mathbb{E} [f(X_T)] \right| \leq Ch
\tag{26}$$

for some constant C , all sufficiently small h and suitably smooth f . It was shown that 26 can be improved to

$$\mathbb{E} \left[f(\hat{X}_T^h) \right] = \mathbb{E} [f(X_T)] + ch + \mathcal{O}(h^2),
\tag{27}$$

where c depends on f .

Applying 27 with discretization step $2h$, we obtain

$$\mathbb{E} \left[f(\hat{X}_T^{2h}) \right] = \mathbb{E} [f(X_T)] + 2ch + \mathcal{O}(h^2),
\tag{28}$$

implying

$$2\mathbb{E} \left[f(\hat{X}_T^{2h}) \right] - \mathbb{E} \left[f(\hat{X}_T^h) \right] = \mathbb{E} [f(X_T)] + \mathcal{O}(h^2),
\tag{29}$$

For higher levels extrapolations, we use the following: Let us denote by $h_J = h_0 \cdot 2^{-J}$ the grid sizes (where h_0 is the coarsest grid size), by K the level of the Richardson extrapolation, and by $I(J, K)$ the approximation of $E[f(\hat{X}_T^{h_J})]$ by terms up to level K (leading to a weak error of order K), then we have

$$(30) \quad I(J, K) = \frac{2^K [I(J, K-1) - I(J-1, K-1)]}{2^K - 1} + \mathcal{O}(h^{K+1}), \quad J = 1, 2, \dots, K = 1, 2, \dots$$

3.6 Root Finding

Without loss of generality, we can assume that the integration domain can be divided into two parts Ω_1 , and Ω_2 such that the integrand f is smooth and positive in Ω_1 whereas $f(\mathbf{x}) = 0$ in Ω_2 . Therefore,

$$(31) \quad If := \int_{\Omega_1} f(\mathbf{x}) d\mathbf{x}$$

This situation may arise when the integrand is non-differentiable or noncontinuous along the boundary between Ω_1 and Ω_2 . For these problems, kinks and jumps can efficiently be identified by a one-dimensional root finding. Then, the kinks and jumps can be transformed to the boundary of integration domain such that they no longer deteriorate the performance of the numerical methods. In fact, we compute the zeros of the integrand with respect to the last dimension. In this dimension, then, e.g., Newton's method or bisection can be used to identify the point which separates Ω_1 and Ω_2 . In our project, we use Newton's iteration solver.

Let us call y the mapping such that: $y : \mathbf{z}_1 \rightarrow z^{\text{kink}}$, where z^{kink} is the "location of irregularity", i.e., g is not smooth at the point $\phi \circ \Phi \circ \Psi(z^{\text{kink}}, \mathbf{z}_{-1})$. Generally, there might be (for given \mathbf{z}_{-1}

- no solution, i.e., the integrand in the definition of $h(\mathbf{z}_{-1})$ above is smooth (*best case*);
- a unique solution;
- multiple solutions.

Generally, we need to assume that we are in the first or second case. Specifically, we need that

$$\mathbf{z}_{-1} \mapsto h(\mathbf{z}_{-1}) \text{ and } \mathbf{z}_{-1} \mapsto \hat{h}(\mathbf{z}_{-1})$$

are smooth, where \hat{h} denotes the numerical approximation of h based on a grid containing $y(\mathbf{z}_{-1})$. In particular, y itself should be smooth in \mathbf{z}_{-1} . This would already be challenging in practice in the third case. Moreover, in the general situation we expect the number of solutions y to increase when the discretization of the SDE gets finer.

In many situations, case 2 (which is thought to include case 1) can be guaranteed by monotonicity (**I think we need to add also the growth condition**). For instance, in the case of one-dimensional SDEs with z_1 representing the terminal value of the underlying Brownian motion (and \mathbf{z}_{-1} representing the Brownian bridge), this can often be seen from the SDE itself. Specifically, if each increment " dX " is increasing in z_1 , no matter the value of X , then the solution X_T must be increasing in z_1 . This is easily seen to be true in examples such as the Black-Scholes model and the

CIR process. (Strictly speaking, we have to distinguish between the continuous and discrete time solutions. In these examples, it does not matter.) On the other hand, it is also quite simple to construct counter examples, where monotonicity fails, for instance SDEs for which the “volatility” changes sign, such as a trigonometric function.¹

Even in multi-dimensional settings, such monotonicity conditions can hold in specific situations. For instance, in case of a basket option in a multivariate Black Scholes framework, we can choose a linear combination z_1 of the terminal values of the driving Bm, such that the basket is a monotone function of z_1 . (The coefficients of the linear combination will depend on the correlations and the weights of the basket.) However, in that case this may actually not correspond to the optimal “rotation” in terms of optimizing the smoothing effect.

3.7 Description of the Domain Decomposition and Suitable Transformation

The payoff function is not smooth due to the nature of the option. In fact, the holder would not exercise the option if a purchase or sale of the underlying asset would lead to a loss. As a result, the discontinuity of the payoff function carries over to the integrand. In this case, The integrand shows a kink or even a jump with respect to a manifold. Since some (mixed) derivatives are not bounded at these manifolds, the smoothness requirements for the sparse grid method are clearly not fulfilled any more.

The first step consists of identifying the areas of discontinuity or non-differentiability. Then, we decompose the total integration domain Ω into sub-domains Ω_i , $i = 1, \dots, n$ such that the integrand is smooth in the interior of Ω_i and such that all kinks and jumps are located along the boundary of these areas. This procedure results in integrating several smooth functions, instead of one discontinuous function. The total integral is then given as the sum of the separate integrals, *i.e.*

$$(32) \quad If := \int_{\Omega} f(\mathbf{x}) d\mathbf{x} = \sum_{i=1}^n \int_{\Omega_i} f(\mathbf{x}) d\mathbf{x}$$

In this way, the fast convergence of SG can be regained whereas the costs only increase by a constant (the number of terms in the sum), provided the cost required for the decomposition is sufficiently small such that it can be neglected.

In general, such a decomposition is even more expensive than to integrate the function. Nevertheless, for some problem classes, the areas of discontinuity have a particular simple form, which allows to decompose the integration domain with costs that are much smaller than the benefit which results from the decomposition. In this work, we consider those cases.

In the literature, there two classes that have been tackled. In the first one, we have the information that the kinks are part of the integration domain where the integrand is zero and can thus be identified by root finding as proposed in [5].

In the second class, we have the information that the discontinuities are located on hyperplanes, which allows a decomposition first into polyhedrons and then into orthants as discussed in [6]. In this work, we start by the first class of problems.

¹Actually, in every such case the simple remedy is to replace the volatility by its absolute value, which does not change the law of the solution. Hence, there does not seem to be a one-dimensional counter-example.

4 Error discussion

4.1 Errors in smoothing

For the analysis it is useful to assume that \hat{h} is a smooth function of \mathbf{z}_{-1} , but in reality this is not going to be true. Specifically, if the true location y of the non-smoothness in the system were available, we could actually guarantee \hat{h} to be smooth, for instance by choosing

$$\hat{h}(\mathbf{z}_{-1}) = \sum_{k=-K}^K \eta_k g(\phi \circ \Phi \circ \Psi(\zeta_k(y(\mathbf{z}_{-1})), \mathbf{z}_{-1})),$$

for points $\zeta_k \in \mathbb{R}$ with $\zeta_0 = y$ and corresponding weights η_k .² However, in reality we have to numerical approximate y by \bar{y} with error $|y - \bar{y}| \leq \delta$. Now, the actual integrand in \mathbf{z}_{-1} becomes

$$\bar{h}(\mathbf{z}_{-1}) := \sum_{k=-K}^K \eta_k g(\phi \circ \Phi \circ \Psi(\zeta_k(\bar{y}(\mathbf{z}_{-1})), \mathbf{z}_{-1})),$$

which we cannot assume to be smooth anymore. On the other hand, if $\zeta_k(y)$ is a continuous function of y and y and \bar{y} are continuous in \mathbf{z}_{-1} , then *eventually* we will have

$$\|\hat{h} - \bar{h}\|_{\infty} \leq \text{TOL}, \quad \|h - \bar{h}\|_{\infty} \leq \text{TOL},$$

i.e., the smooth functions h and \hat{h} are close to the integrand \bar{h} . (Of course, this may depend on us choosing a good enough quadrature ζ !)

Remark 4.1. If the adaptive collocation used for computing the integral of \bar{h} depends on derivatives (or difference quotients) of its integrand \bar{h} , then we may also need to make sure that derivatives of \bar{h} are close enough to derivatives of \hat{h} or h . This may require higher order solution methods for determining y .

Remark 4.2. In some important cases, f may be trivial (e.g., $\equiv 0$). In these cases, we may be able to make sure that \bar{y} never crosses the “location of non-smoothness”. Then even \bar{h} is smooth.

Remark 4.3. We expect that the global error of our procedure will be bounded by the weak error which is in our case of order $O(\Delta t)$. In this case, the overall complexity of our procedure will be of order $O(\text{TOL}^{-1})$. We note that this rate can be improved up to $O(\text{TOL}^{-\frac{1}{2}})$ if we use **Richardson extrapolation**. Another way that can improve the complexity could be based on **Cubature on Wiener Space** (This is left for a future work). The aimed complexity rate illustrates the contribution of our procedure which outperforms Monte Carlo forward Euler (MC-FE) and multi-level MC-FE, having complexity rates of order $O(\text{TOL}^{-3})$ and $O(\text{TOL}^{-2} \log(\text{TOL})^2)$ respectively.

Remark 4.4.

We need to check the impact of the error caused by the Newton iteration on the integration error. In the worst case, we expect that if the error in the Newton iteration is of order $O(\epsilon)$ than the integration error will be of order $\log(\epsilon)$. But we need to check that too.

²Of course, the points ζ_k have to be chosen in a systematic manner depending on y .

5 Numerical experiments

5.1 The discretized 1D Black-Scholes

The first two examples that we will test later are the single binary and call options under BS model where the process X is the discretized one dimensional Black-Scholes model and the payoff function g is the indicator or maximum function, and which has a kink. Precisely, we are interested in the 1-d lognormal example where the dynamics of the stock are given by

$$(33) \quad dX_t = \sigma X_t dB_t,$$

where $\{B_t, 0 \leq t \leq T\}$ is a standard one-dimensional Brownian motion. In the discrete case, the numerical approximation of $X(T)$, using N time steps ($\Delta t = \frac{T}{N}$), satisfies

$$(34) \quad \begin{aligned} \bar{X}_T &= \Phi(\Delta t, z_1, \Delta B_0, \dots, \Delta B_{N-1}), \\ &= \Phi(\Delta t, \Psi(z_1, \dots, z_N)), \end{aligned}$$

where (z_1, \dots, z_N) are standard Gaussian random variables, for some path function Φ and Brownian bridge map Ψ as described in Section 3.4.1.

As explained in Section 3, the first step of our approach is determining the location of irregularity (kink). In the following, we want to compare different ways for identifying the location of the kink for this model.

5.1.1 Determining the kink location

Exact location of the kink for the continuous problem

Let us denote y_* an invertible function that satisfies

$$(35) \quad X(T; y_*(x), B) = x.$$

We can easily prove that the expression of y_* for model given by (33) is given by

$$(36) \quad y_*(x) = (\log(x/x_0) + T\sigma^2/2) \frac{1}{\sqrt{T}\sigma},$$

and since the kink for Black-Scholes model occurs at $x = K$, where K is the strike price then the exact location of the continuous problem is given by

$$(37) \quad y_*(K) = (\log(K/x_0) + T\sigma^2/2) \frac{1}{\sqrt{T}\sigma}.$$

Exact location of the kink for the discrete problem

The discrete problem of model (33) is solved by simulating

$$\begin{aligned}
 X_{t_1} &= X_{t_0} \left[1 + \frac{\sigma}{\sqrt{T}} z_1 \Delta t + \sigma \Delta B_0 \right] \\
 X_{t_2} &= X_{t_1} \left[1 + \frac{\sigma}{\sqrt{T}} z_1 \Delta t + \sigma \Delta B_1 \right] \\
 &\vdots \\
 X_{t_N} &= X_{t_{N-1}} \left[1 + \frac{\sigma}{\sqrt{T}} z_1 \Delta t + \sigma \Delta B_{N-1} \right]
 \end{aligned}
 \tag{38}$$

implying that

$$\bar{X}(T) = X_0 \prod_{i=0}^{N-1} \left[1 + \frac{\sigma}{\sqrt{T}} z_1 \Delta t + \sigma \Delta B_i \right].
 \tag{39}$$

Therefore, in order to determine y_* , we need to solve

$$x = \bar{X}(T; y_*, B) = X_0 \prod_{i=0}^{N-1} \left[1 + \frac{\sigma}{\sqrt{T}} y_*(x) \Delta t + \sigma \Delta B_i \right],
 \tag{40}$$

which implies that the location of the kink point for the approximate problem is equivalent to finding the roots of the polynomial $P(y_*(K))$, given by

$$P(y_*(K)) = \prod_{i=0}^{N-1} \left[1 + \frac{\sigma}{\sqrt{T}} y_*(K) \Delta t + \sigma \Delta B_i \right] - \frac{K}{X_0}.
 \tag{41}$$

The exact location of the kink can be obtained exactly by solving exactly $P(y_*(K)) = 0$.

Approximate location of the discrete problem

Here, we try to find the roots of polynomial $P(y_*(K))$, given by (41), by using **Newton iteration method**. In this case, we need the expression $P' = \frac{dP}{dy_*}$. If we denote $f_i(y) = 1 + \frac{\sigma}{\sqrt{T}} y \Delta t + \sigma \Delta B_i$, then we can easily show that

$$P'(y) = \frac{\sigma \Delta t}{\sqrt{T}} \left(\prod_{i=0}^{N-1} f_i(y) \right) \left[\sum_{i=0}^{N-1} \frac{1}{f_i(y)} \right]
 \tag{42}$$

Therefore, in this case, the integrand $h(\mathbf{z}_{-1})$ (as expressed in (13)) is given by

$$h(\mathbf{z}_{-1}) = \int_{\Omega} \max [(\Phi \circ \Psi(T; z_1, \mathbf{z}_{-1})) - K, 0] \rho_1(z_1) dz_1.
 \tag{43}$$

We get the kink point by running Newton iteration for root solving of the polynomial P as expressed in (41) with a precision of 10^{-10} . We decompose the total integration domain Ω into

sub-domains Ω_i , $i = 1, 2$ such that the integrand is smooth in the interior of Ω_i and such that the kink is located along the boundary of these areas. The total integral is then given as the sum of the separate integrals, *i.e.*

$$(44) \quad \begin{aligned} h(\mathbf{z}_{-1}) &:= \int_{\Omega} \max [(\Phi \circ \Psi(T; z_1, \mathbf{z}_{-1})) - K, 0] \rho_1(z_1) dz_1 \\ &= \sum_{i=1}^2 \int_{\Omega_i} \max [(\Phi \circ \Psi(T; z_1, \mathbf{z}_{-1})) - K, 0] \rho_d(z_1) dz_1, \end{aligned}$$

where we use Gauss-laguerre quadrature with β points to get each part.

5.2 The basket call option under the discretized multi-dimensional Black-Scholes

In the following, I present two ways of solving the root finding problem in multi-dimension. The first way, presented in Section 5.2.1, is an extension of Section 5.1, and the numerical results in Section 5.6 are based on applying this way of numerical smoothing. In the second way, presented in Section 5.2.2, we tried a different approach that is inspired by the work of [2].

5.2.1 First way

In this suggested way, I try to extend the way we solved the one dimensional problem, as in Section 5.1, to higher dimensions.

We consider the basket option under multi-dimensional BS model where the process \mathbf{X} is the discretized d -dimensional Black-Scholes model and the payoff function g is given by

$$(45) \quad g(\mathbf{X}(T)) = \max \left(\sum_{i=1}^d \omega_i X^{(i)}(T) - K, 0 \right)$$

Precisely, we are interested in the d -dimensional lognormal example where the dynamics of the stock are given by

$$(46) \quad dX_t^{(i)} = \sigma^{(i)} X_t^{(i)} dB_t^{(i)},$$

where $\{B^{(1)}, \dots, B^{(d)}\}$ are correlated Brownian motions with correlations ρ_{ij} .

In the discrete case, the numerical approximation of $X^{(j)}(T)$ satisfies

$$(47) \quad \begin{aligned} \bar{X}_T^{(j)} &= \Phi(\Delta t, z_1^{(j)}, \Delta B_0^{(j)}, \dots, \Delta B_{N-1}^{(j)}), \quad 1 \leq j \leq d, \\ &= \Phi(\Delta t, \Psi(z_1^{(j)}, \dots, z_N^{(j)})), \quad 1 \leq j \leq d, \end{aligned}$$

for some path function Φ and Brownian bridge map Ψ as described in Section 3.4.1.

Using results from section 5.1, we have

$$(48) \quad \bar{X}^{(j)}(T) = X_0^{(j)} \prod_{i=0}^{N-1} \left[1 + \frac{\sigma^{(j)}}{\sqrt{T}} z_1^{(j)} \Delta t + \sigma^{(j)} \Delta B_i^{(j)} \right], \quad 1 \leq j \leq d.$$

Therefore, in order to determine $\mathbf{y}_* = (y_*^{(1)}, \dots, y_*^{(d)})$, we need to solve

$$(49) \quad \mathbf{x} = \sum_{j=1}^d \omega_j X_0^{(j)} \prod_{i=0}^{N-1} \left[1 + \frac{\sigma^{(j)}}{\sqrt{T}} y_*^{(j)}(\mathbf{x}) \Delta t + \sigma^{(j)} \Delta B_i^{(j)} \right],$$

which implies that the location of the kink point for the approximate problem is equivalent to finding the roots of the polynomial $P(\mathbf{y}_*(K))$, given by

$$(50) \quad \begin{aligned} P(\mathbf{y}_*(K)) &= \sum_{j=1}^d \omega_j X_0^{(j)} \prod_{i=0}^{N-1} \left[1 + \frac{\sigma^{(j)}}{\sqrt{T}} y_*^{(j)} \Delta t + \sigma^{(j)} \Delta B_i^{(j)} \right] - K, \\ &= \sum_{j=1}^d \omega_j X_0^{(j)} \left(\prod_{i=0}^{N-1} \left[1 + \frac{\sigma^{(j)}}{\sqrt{T}} y_*^{(j)} \Delta t + \sigma^{(j)} \Delta B_i^{(j)} \right] - \frac{K}{\omega_j X_0^{(j)} d} \right) \\ &= \sum_{j=1}^d \omega_j X_0^{(j)} P^{(j)} \left(y_*^{(j)} \left(\frac{K}{\omega_j X_0^{(j)} d} \right) \right) \end{aligned}$$

Therefore, the problem of finding the kink in the d -dimensional problem is brought to finding the location of the kink for each dimension by solving the root of the polynomial $P^{(j)} \left(y_*^{(j)} \left(\frac{K}{\omega_j X_0^{(j)} d} \right) \right)$.

Using **Newton iteration method**, we use the expression $P' = \frac{dP^{(j)}}{dy_*^{(j)}}$. If we denote $f_i^{(j)}(y) = 1 + \frac{\sigma^{(j)}}{\sqrt{T}} y \Delta t + \sigma^{(j)} \Delta B_i^{(j)}$, then we can easily show that

$$(51) \quad P'^{(j)}(y) = \frac{\sigma^{(j)} \Delta t}{\sqrt{T}} \left(\prod_{i=0}^{N-1} f_i^{(j)}(y) \right) \left[\sum_{i=0}^{N-1} \frac{1}{f_i^{(j)}(y)} \right].$$

Therefore, in this case, the integrand $h(\mathbf{z}_{-1}^{(1)}, \dots, \mathbf{z}_{-1}^{(d)})$ (as expressed in (17)) is given by

$$(52) \quad h(\mathbf{z}_{-1}^{(1)}, \dots, \mathbf{z}_{-1}^{(d)}) = \int_{\Omega} \max \left[\left(\sum_{j=1}^d \Phi \circ \Psi(T; z_1^{(j)}, \mathbf{z}_{-1}^{(j)}) \right) - K, 0 \right] \rho_d(z_1^{(1)}, \dots, z_1^{(d)}) dz_1^{(1)} \dots dz_1^{(d)}.$$

We get the kink point by running Newton iteration in each dimension separately for root solving of each polynomial $P^{(j)}$ as expressed in (50) with a precision of 10^{-10} . We decompose the total integration domain Ω into sub-domains Ω_i , $i = 1, 2, \dots, 2^d$ such that the integrand is smooth in the interior of Ω_i and such that the kink is located along the boundary of these areas. The total integral is then given as the sum of the separate integrals, *i.e.*

$$(53) \quad \begin{aligned} h(\mathbf{z}_{-1}^{(1)}, \dots, \mathbf{z}_{-1}^{(d)}) &:= \int_{\Omega} \max \left[\left(\sum_{j=1}^d \Phi \circ \Psi(T; z_1^{(j)}, \mathbf{z}_{-1}^{(j)}) \right) - K, 0 \right] \rho_d(z_1^{(1)}, \dots, z_1^{(d)}) dz_1^{(1)} \dots dz_1^{(d)} \\ &= \sum_{i=1}^{2^d} \int_{\Omega_i} \max \left[\left(\sum_{j=1}^d \Phi \circ \Psi(T; z_1^{(j)}, \mathbf{z}_{-1}^{(j)}) \right) - K, 0 \right] \rho_d(z_1^{(1)}, \dots, z_1^{(d)}) dz_1^{(1)} \dots dz_1^{(d)}, \end{aligned}$$

where we use Gauss-laguerre quadrature with β points to get each part.

5.2.2 Second way

The i -th asset $X^{(i)}$ of the basket ($i = 1, \dots, d$) is given by

$$(54) \quad X_{k\Delta t}^{(i)} = X_0^{(i)} \exp \left(-\frac{\sigma_i^2}{2} k\Delta t + \sigma_i B_{k\Delta t}^{(i)} \right), \quad 1 \leq k \leq N,$$

where $X_0^{(i)}$ is the current price of the i -th asset, σ_i is the volatility of the i -th asset and $B = (B^{(1)}, \dots, B^{(d)})$ is a d -dimensional Brownian motion. The correlation between $B^{(i)}$ and $B^{(j)}$ is denoted by ρ_{ij} . The payoff function of the European basket option is given by

$$(55) \quad f(Z) = \max \left(\sum_{i=1}^d c_i X_T^{(i)}(Z) - K, 0 \right),$$

where c_i is the corresponding weight of the i -th asset, $Z \in \mathbb{R}^{N \times d}$ is standard Gaussian vector, and

$$(56) \quad X_{k\Delta t}^{(i)}(Z) = X_0^{(i)} e^{-\frac{\sigma_i^2}{2} k\Delta t} \exp \left(\sum_{j=1}^{dN} C_{(k-1)d+i,j} Z_j \right).$$

where C is a $dN \times dN$ -matrix with $CC^T = \tilde{\Sigma} := R \otimes \Sigma$, and R is an $d \times d$ -matrix with $R_{ij} = \sqrt{T/N} \rho_{ij} \sigma_i \sigma_j$.

Therefore, we have

$$(57) \quad \begin{aligned} X_T^{(i)}(Z) &= X_{N\Delta t}^{(i)}(Z) = X_0^{(i)} e^{-\frac{\sigma_i^2}{2} T} \exp \left(\sum_{j=1}^{dN} C_{(N-1)d+i,j} Z_j \right) \\ &= w^{(i)} \exp(A_{i*} Z), \end{aligned}$$

where $w^{(i)} = X_0^{(i)} e^{-\frac{\sigma_i^2}{2} T}$, A is a $d \times dN$ matrix such that $A := (C_{(N-1)d+i,j})_{1 \leq i \leq d, 1 \leq j \leq dN}$, and A_{i*} is the i -th row vector of A .

Going back to (55), we have

$$\begin{aligned}
f(Z) &= \max \left(\sum_{i=1}^d c_i S_T^{(i)}(Z) - K, 0 \right) \\
&= \max \left(\sum_{i=1}^d w_i \exp \left(\sum_{j=1}^{dN} C_{(N-1)d+i,j} Z_j \right) - K, 0 \right) \\
&= \max \left(\sum_{i=1}^d w_i \left(\exp \left(\sum_{\ell=1}^d C_{(N-1)d+i,(\ell-1)N+1} Z_{(\ell-1)N+1} + \sum_{\substack{j=1 \\ j \neq (\ell-1)N+1, 1 \leq \ell \leq d}}^{dN} C_{(N-1)d+i,j} Z_j \right) \right) - K, 0 \right) \\
&= \max \left(\sum_{i=1}^d w_i \exp(y_i) \exp \left(\sum_{\substack{j=1 \\ j \neq (\ell-1)N+1, 1 \leq \ell \leq d}}^{dN} C_{(N-1)d+i,j} Z_j \right) - K, 0 \right) \\
(58) \quad &= \max \left(\sum_{i=1}^d w_i \exp(y_i) h_i(\mathbf{Z}_{-1}^{(1)}, \dots, \mathbf{Z}_{-1}^{(d)}) - K, 0 \right),
\end{aligned}$$

where

$$\begin{aligned}
w_i &= c_i X_0^{(i)} e^{-\frac{\sigma_i^2}{2} T} \\
y_i &= \sum_{\ell=1}^d C_{(N-1)d+i,(\ell-1)N+1} Z_{(\ell-1)N+1} \\
h_i(\mathbf{Z}_{-1}^{(1)}, \dots, \mathbf{Z}_{-1}^{(d)}) &= \exp \left(\sum_{\substack{j=1 \\ j \neq (\ell-1)N+1, 1 \leq \ell \leq d}}^{dN} C_{(N-1)d+i,j} Z_j \right).
\end{aligned}$$

y_i can be seen always as a linear combination including the first factors in each asset dimension.

Giving the representation given by (58), it seems to me that we need first to solve root finding problem wrt $\{y_i\}_{i=1}^d$, then giving $\{y_i^*\}_{i=1}^d$, we get the kink locations $\{Z_{N(i-1)+1}^*\}_{i=1}^d$ by solving a d -dimensional system.

Another way maybe to solve the problem is to mimic the methodology in [2]. In fact,

5.3 Summary of numerical results

We conduct our experiments for 3 different examples under discretized BS model: i) single Binary, ii) single Call, and basket call options (We just included results for 2-dimensional basket, I still have issue for higher dimensions that we need to discuss, and this is maybe related to the way I am solving the problem in high dimension).

In Sections 5.4.1, 5.5.1 and 5.6.1, we estimate the weak error (Bias) of MC combined with root finding, for the different examples, for 2 scenarios involving with/without Richardson extrapolation. The conclusions of this section are:

- Without Richardson extrapolation: For all cases, we get a weak error of order Δt , with different constants. Interestingly, for the call example, we needed to increase the number of quadrature points sufficiently, used for Laguerre quadrature, to observe the right behavior of the weak error (See tables (2, 12,22) for the corresponding bias values as well the statistical errors.).
- With Richardson extrapolation: For the case of binary and 2-dimensional basket call options, we get a weak error of order almost Δt^2 . For the case of single call, we get a weak error of order higher than Δt^2 (See tables (7,17, 27) for the corresponding bias values as well the statistical errors.).

Remark 5.1. We emphasize that the reported weak rates correspond to the pre-asymptotic regime that we are interested in. We are not interested on estimating the rates specifically but rather a sufficient precise estimate of the weak error (Bias), $\mathcal{E}_B(N)$, for different time steps N , in order to get the biased MC solution for a given discretization, that we denoted $Q^N(\infty)$ in Section 3.3. For a fixed discretization, the corresponding biased solution will be set as a reference solution to the MISC solver in order to estimate the quadrature error $\mathcal{E}_Q(TOL_{\text{MISC}}, N)$.

In Sections 5.4.2, 5.5.2 and 5.6.2, we show tables and plots reporting the different errors involved in MC method (bias and statistical error), and in MISC (Quadrature error). The quadrature error (see (23)) is computed by subtracting the MISC solution from the biased solution, computed with sufficiently large number of samples (to kill the statistical error). Given that both methods, MC and MISC, have the same bias, the computational time of MC and MISC is compared such that the statistical error is almost equal to the stable quadrature error produced by MISC.

The conclusions of those sections are:

- The Quadrature error of MISC is very stable with respect to TOL_{MISC} , for all cases. (See figures (12,3,14,5)).
- MISC is outperforming significantly MC and MC+root finding methods. The ratio of gain is more significant for the Call option compared to Binary option (See tables (5,10,15)). See also figures (4,6,13) for the comparison of complexity for different methods.
- Richardson extrapolation has a great advantage over the rate as well the constant for complexity of MISC:
 - For the binary case: we may see from figure 7 and tables (4,5,9,10), that without using Richardson extrapolation, with 16 time steps, we achieve 1.4% of total relative error, with a cost of 1090 of CPU time. This cost is dramatically decreased when using Richardson extrapolation. In fact, with 16 steps in the finer level, we only pay 42 of CPU time to get a total relative error of 0.3%.
 - For the Call case: we may see from figure 15 and tables (14,15,19,20), that without using Richardson extrapolation, with 16 time steps, we achieve 0.46% of total relative error, with a cost of 656 of CPU time. This cost is dramatically decreased when using Richardson extrapolation. In fact, with 8 steps in the finer level, we only pay 135 of CPU time to get a total relative error of 0.25%.

5.4 Results for the single binary option example

In this case, the integrand $h(\mathbf{z}_{-1})$ is given by

$$(59) \quad \begin{aligned} h(\mathbf{z}_{-1}) &= \int \mathbf{1}_{\Phi \circ \Psi(T; z_1, \mathbf{z}_{-1}) > K} \frac{1}{\sqrt{2\pi}} \exp(-z_1^2/2) dy \\ &= P(Y > y_*(K)), \end{aligned}$$

where $y_*(x)$, is an invertible function that satisfies

$$(60) \quad \Phi \circ \Psi(T; y_*(x), \mathbf{z}_{-1}) = x$$

We get the kink point by running Newton iteration with a precision of 10^{-10} .

The paramters that we used in our numerical experiments are: $T = 1$, $\sigma = 0.4$ and $S_0 = K = 100$. The exact value of this case is 0.42074029.

5.4.1 Weak error plots

In this section, we include the results of weak error rates, for the binary option example, for 2 scenarios, without/with Richardson extrapolation (level 1). We note that the weak errors plotted here correspond to relative errors. The upper and lower bounds are 95% confidence interval.

From figure 1, we see that we get a weak error of order Δt . From figure 2, we observe an improvement in the rate and the constant when using level 1 of Richardson extrapolation. The corresponding values of the Bias are reported in tables (2,7).

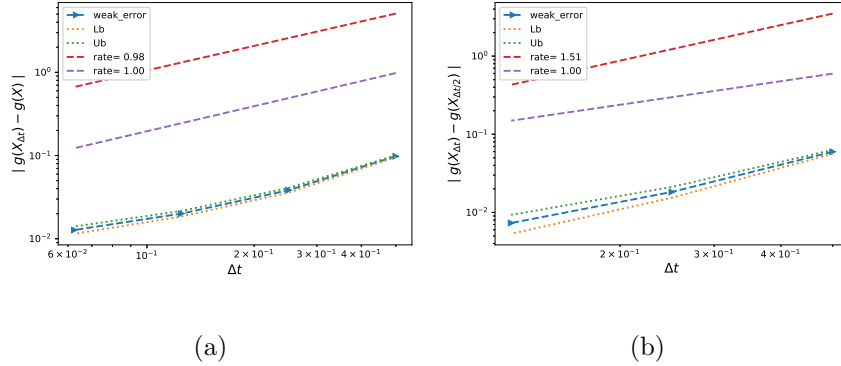


Figure 1: The rate of convergence of the weak error for the binary option, without Richardson extrapolation, using MC with $M = 10^4$: a) $|E[g(X_{\Delta t})] - g(X)|$ b) $|E[g(X_{\Delta t}) - g(X_{\Delta t/2})]|$

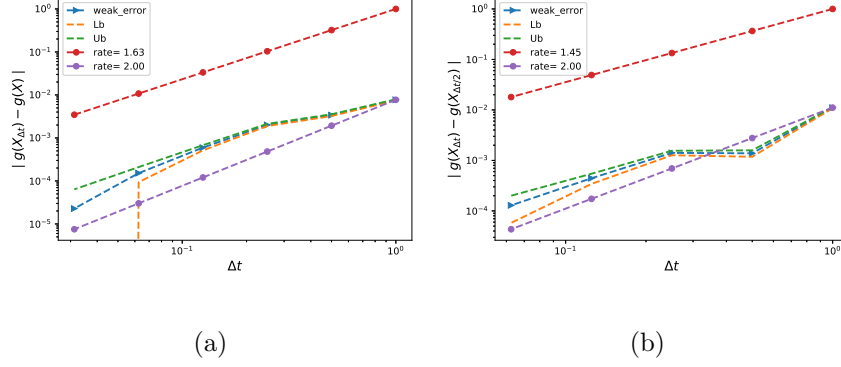


Figure 2: The rate of convergence of the weak error for the binary option, with Richardson extrapolation (level 1), using MC with $M = 5.10^6$: a) $|E[2g(X_{\Delta t/2}) - g(X_{\Delta t})] - g(X)|$ b) $|E[3g(X_{\Delta t/2}) - g(X_{\Delta t}) - 2g(X_{\Delta t/4})]|$

5.4.2 Comparing relative errors

Without Richardson extrapolation

In this Section, we report the results for the binary option, using the different Methods: MISC, MC + root finding and MC, without Richardson extrapolation. We mention that for MISC we used a very small tolerance for the Newton solver, when solving the Kink point problem ($TOL_{\text{Newton}} = 10^{-10}$). We start by reporting the observed approximated values using different methods (See table 1. The biased values for MC method were computed using the values of Bias, reported in table 2. In table 3, we report the behavior of quadrature error with respect to MISC tolerance. We precise that the quadrature error is computed by subtracting the MISC approximated value from the biased MC value. We report in red the values where MISC becomes stable (see also figure 3). Those values were used to compute the needed number of samples for MC (with and without root finding), to achieve similar magnitude for statistical error. Later, in table 4, we report the total relative error for all methods (Quadrature error + Bias for MISC and Statistical error + Bias for MC). We also report in table 5, the computational time needed for all different methods. We finally provide in figure 4, the complexity rates for the different involved methods.

Method \ Steps	2	4	8	16
MISC ($Tol = 5.10^{-1}$)	0.4620	0.4404	0.4299	0.4250
MISC ($Tol = 10^{-1}$)	0.4620	0.4404	0.4301	0.4250
MISC ($Tol = 5.10^{-2}$)	0.4620	0.4403	0.4300	0.4250
MISC ($Tol = 10^{-2}$)	0.4620	0.4406	0.4300	0.4250
MISC ($Tol = 10^{-3}$)	0.4620	0.4406	0.4301	0.4254
MISC ($Tol = 10^{-4}$)	0.4620	0.4406	0.4301	—
MC method ($M = 10^4$)	0.4620	0.4369	0.4292	0.4261

Table 1: Binary option price of the different methods for different number of time steps, without Richardson extrapolation.

Method \ Steps	2	4	8	16
MC Bias ($M = 10^4$)	0.0980 (0.0412)	0.0384 (0.0162)	0.0201 (0.0085)	0.0127 (0.0053)
MC Statistical error ($M = 10^4$)	1.2e - 03 (5.0e-04)	1.2e - 03 (5.0e-04)	8.0e - 04 (3.4e-04)	6.5e - 04 (2.7e-04)

Table 2: Bias and Statistical errors of MC for computing Binary option price for different number of time steps, without Richardson extrapolation. The numbers between parentheses are the corresponding absolute errors.

Method \ Steps	2	4	8	16
MISC ($Tol = 5.10^{-1}$)	1.0e - 05 (2.4e-05)	0.0083 (0.0035)	0.0017 (0.0007)	0.0026 (0.0011)
MISC ($Tol = 10^{-1}$)	1.0e - 05 (2.4e-05)	0.0083 (0.0035)	0.0021 (0.0009)	0.0026 (0.0011)
MISC ($Tol = 5.10^{-2}$)	1.0e - 05 (2.4e-05)	0.0081 (0.0034)	0.0019 (0.0008)	0.0026 (0.0011)
MISC ($Tol = 10^{-2}$)	1.0e - 05 (2.4e-05)	0.0088 (0.0037)	0.0019 (0.0008)	0.0026 (0.0011)
MISC ($Tol = 10^{-3}$)	1.0e - 05 (2.4e-05)	0.0088 (0.0037)	0.0021 (0.0009)	0.0017 (0.0007)
MISC ($Tol = 10^{-4}$)	1.0e - 05 (2.4e-05)	0.0088 (0.0037)	0.0021 (0.0009)	— (—)

Table 3: Quadrature error of MISC to compute Binary option price of the different tolerances for different number of time steps, without Richardson extrapolation. The numbers between parentheses are the corresponding absolute errors.

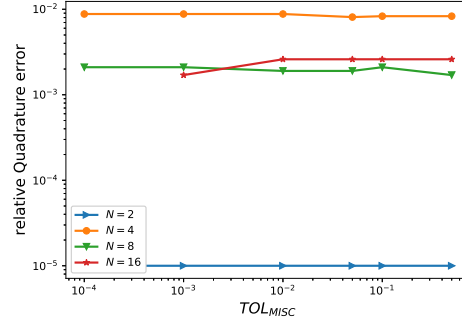


Figure 3: Relative quadrature error of MISC to compute Binary option price of the different tolerances for different number of time steps, without Richardson extrapolation.

Method \ Steps	2	4	8	16
MISC ($Tol = 5 \cdot 10^{-1}$)	0.0980	0.0467	0.0218	0.0153
MISC ($Tol = 10^{-1}$)	0.0980	0.0467	0.0222	0.0153
MISC ($Tol = 5 \cdot 10^{-2}$)	0.0980	0.0465	0.0220	0.0153
MISC ($Tol = 10^{-2}$)	0.0980	0.0472	0.0220	0.0153
MISC ($Tol = 10^{-3}$)	0.0980	0.0472	0.0222	0.0144
MISC ($Tol = 10^{-4}$)	0.0980	0.0472	0.0222	—
MC+root finding	—	0.0471	0.0221	0.0141
MC	—	0.0467	0.0222	0.0146

Table 4: Total error of MISC and MC to compute Binary option price of the different tolerances for different number of time steps, without Richardson extrapolation. The numbers between parentheses are the corresponding absolute errors. We will not include later the first point, corresponding to number of time steps $N = 2$, since as from table 3, MISC is killing the quadrature error for that case.

Method \ Steps	2	4	8	16
MISC ($Tol = 5 \cdot 10^{-1}$)	0.3	0.8	2	9
MISC ($Tol = 10^{-1}$)	0.3	0.8	9	49
MISC ($Tol = 5 \cdot 10^{-2}$)	0.3	1.3	12	59
MISC ($Tol = 10^{-2}$)	0.3	2	14	63
MISC ($Tol = 10^{-3}$)	0.3	2	34	1090
MISC ($Tol = 10^{-4}$)	0.3	16	193	—
MC+root finding method	—	9	96	141
MC method	—	7	95	152
Ratio of (MC+root finding)/(MISC)	—	4.5	11	0.13
Ratio of (MC)/(MISC)	—	3.5	11	0.14

Table 5: Comparson of the computational time of MC and MISC, used to compute Binary option price for different number of time steps, without Richardson extrapolation. The average computational time of MC is computed over 10 runs.

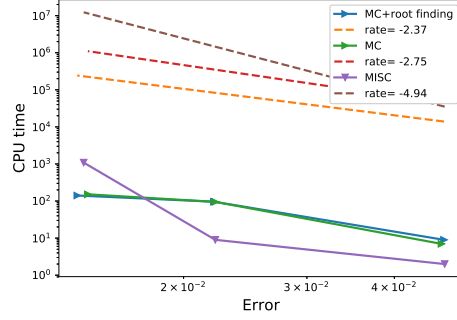


Figure 4: Complexity plot for MC and MISC for the case without Richardson extrapolation.

With Richardson extrapolation (level 1)

In this Section, we report the results for the binary option, using the different Methods: MISC, MC + root finding and MC, with Richardson extrapolation. We mention that for MISC we used a very small tolerance for the Newton solver, when solving the Kink point problem ($TOL_{\text{Newton}} = 10^{-10}$). We start by reporting the observed approximated values using different methods (See table 6. The biased values for MC method were computed using the values of Bias, reported in table 7. In table 8, we report the behavior of quadrature error with respect to MISC tolerance. We precise that the quadrature error is computed by subtracting the MISC approximated value from the biased MC value. We report in red the values where MISC becomes stable (see also figure 5). Those values were used to compute the needed number of samples for MC (with and without root finding), to achieve similar magnitude for statistical error. Later, in table 9, we report the total relative error for all methods (Quadrature error + Bias for MISC and Statistical error + Bias for MC). We also report in table 10, the computational time needed for all different methods. We finally provide in figure 6, the complexity rates for the different involved methods, as well a comparison between the two versions of MISC (without/with Richardson extrapolation) in figure 7.

Method \ Steps	1 – 2	2 – 4	4 – 8	8 – 16
MISC ($Tol = 5.10^{-1}$)	0.4239	0.4188	0.4191	0.4200
MISC ($Tol = 10^{-1}$)	0.4239	0.4188	0.4191	0.4199
MISC ($Tol = 5.10^{-2}$)	0.4239	0.4188	0.4190	0.4199
MISC ($Tol = 10^{-2}$)	0.4239	0.4192	0.4194	0.4199
MISC ($Tol = 10^{-3}$)	0.4239	0.4192	0.4199	0.4205
MISC ($Tol = 10^{-4}$)	0.4239	0.4193	0.4199	–
MC method ($M = 5.10^6$)	0.4240	0.4224	0.4216	0.4210

Table 6: Binary option price of the different methods for different number of time steps, with Richardson extrapolation (level 1).

Method \ Steps	1 – 2	2 – 4	4 – 8	8 – 16
MC Bias ($M = 5.10^6$)	0.0077 (0.0032)	0.0039 (0.0016)	0.0020 (0.0008)	0.0006 (0.0003)
MC Statistical error ($M = 5.10^6$)	1.1e – 04 (4.6e–05)	8.4e – 05 (3.5e–05)	6.0e – 05 (2.5e–05)	4.2e – 05 (1.8e–05)

Table 7: Bias and Statistical errors of MC for computing Binary option price for different number of time steps, with Richardson extrapolation (level 1). The numbers between parentheses are the corresponding absolute errors.

Method \ Steps	1 – 2	2 – 4	4 – 8	8 – 16
MISC ($TOL = 5.10^{-1}$)	2.4e – 04 (1.0e–04)	8.6e – 03 (3.6e–03)	5.9e – 03 (2.5e–03)	2.4e – 03 (1.0e–03)
MISC ($TOL = 10^{-1}$)	2.4e – 04 (1.0e–04)	8.6e – 03 (3.6e–03)	5.9e – 03 (2.5e–03)	2.6e – 03 (1.1e–04)
MISC ($TOL = 5.10^{-2}$)	2.4e – 04 (1.0e–04)	8.6e – 03 (3.6e–03)	6.2e – 03 (2.6e–03)	2.6e – 03 (1.1e–04)
MISC ($TOL = 10^{-2}$)	2.4e – 04 (1.0e–04)	7.6e – 03 (3.2e–03)	5.2e – 03 (2.2e–03)	2.6e – 03 (1.1e–04)
MISC ($TOL = 10^{-3}$)	2.4e – 04 (1.0e–04)	7.6e – 03 (3.2e–03)	4.0e – 03 (1.7e–03)	1.2e – 03 (5.e–04)
MISC ($TOL = 10^{-4}$)	2.4e – 04 (1.0e–04)	7.4e – 03 (3.1e–03)	4.0e – 03 (1.7e–03)	()

Table 8: Quadrature error of MISC to compute Binary option price of the different tolerances for different number of time steps, with Richardson extrapolation (level 1). The numbers between parentheses are the corresponding absolute errors.

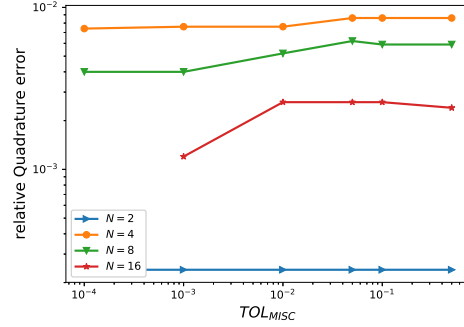


Figure 5: Relative quadrature error of MISC to compute Binary option price of the different tolerances for different number of time steps, with Richardson extrapolation.

Method \ Steps	1 – 2	2 – 4	4 – 8	8 – 16
MISC ($Tol = 5 \cdot 10^{-1}$)	0.0079	0.0125	0.0079	0.0030
MISC ($Tol = 10^{-1}$)	0.0079	0.0125	0.0079	0.0032
MISC ($Tol = 5 \cdot 10^{-2}$)	0.0079	0.0125	0.0082	0.0032
MISC ($Tol = 10^{-2}$)	0.0079	0.0115	0.0072	0.0032
MISC ($Tol = 10^{-3}$)	0.0079	0.0115	0.0060	0.0018
MISC ($Tol = 10^{-4}$)	0.0079	0.0113	0.0060	–
MC+root finding	–	0.0111	0.0070	0.0035
MC	–	0.0116	0.0073	0.0029

Table 9: Total error of MISC and MC to compute Binary option price of the different tolerances for different number of time steps, with Richardson extrapolation (level 1). The numbers between parentheses are the corresponding absolute errors. We will not include later the first point, corresponding to number of time steps $N = 2$, since as from table 8, MISC is killing the quadrature error for that case.

Method \ Steps	1 – 2	2 – 4	4 – 8	8 – 16
MISC ($Tol = 5 \cdot 10^{-1}$)	0.3	1	4	9
MISC ($Tol = 10^{-1}$)	0.3	1	8	42
MISC ($Tol = 5 \cdot 10^{-2}$)	0.3	1	10	72
MISC ($Tol = 10^{-2}$)	0.3	4	15	78
MISC ($Tol = 10^{-3}$)	0.3	4	100	2253
MISC ($Tol = 10^{-4}$)	0.3	68	392	
MC+root finding method	–	48	62	122
MC	–	12	23	147
Ratio of (MC+root finding)/(MISC)	–	12	4.1	2.9
Ratio of (MC)/(MISC)	–	3	1.5	3.5

Table 10: Comparision of the computational time of MC and MISC, used to compute Binary option price for different number of time steps, with Richardson extrapolation (level 1). The average computational time of MC is computed over 10 runs.

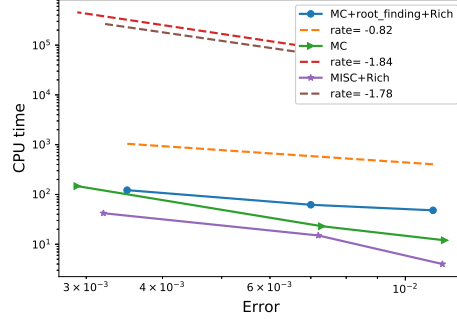


Figure 6: Complexity plot for MC and MISC for the case with Richardson extrapolation.

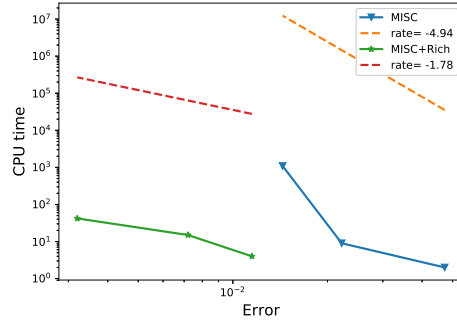


Figure 7: Complexity plot for MISC without and with Richardson extrapolation, for the Binary option.

5.5 Results for the single call option example

In this case, the integrand $h(\mathbf{z}_{-1})$ is given by

$$(61) \quad h(\mathbf{z}_{-1}) = \int_{\Omega} \max(\Phi \circ \Psi(T; z_1, \mathbf{z}_{-1}) - K, 0) \frac{1}{\sqrt{2\pi}} \exp(-z_1^2/2) dz_1$$

We get the kink point by running Newton iteration with a precision of 10^{-10} . We decompose the total integration domain Ω into sub-domains Ω_i , $i = 1, 2$ such that the integrand is smooth in the interior of Ω_i and such that the kink is located along the boundary of these areas. The total integral is then given as the sum of the separate integrals, *i.e.*

$$(62) \quad \begin{aligned} h(\mathbf{z}_{-1}) &:= \int_{\Omega} \max(\Phi \circ \Psi(T; z_1, \mathbf{z}_{-1}) - K, 0) \frac{1}{\sqrt{2\pi}} \exp(-z_1^2/2) dy \\ &= \sum_{i=1}^2 \int_{\Omega_i} \max(\Phi \circ \Psi(T; z_1, \mathbf{z}_{-1}) - K, 0) \frac{1}{\sqrt{2\pi}} \exp(-z_1^2/2) dz_1, \end{aligned}$$

where we use Gauss-laguerre quadrature with β points to get each part.

The parameters that we used in our numerical experiments are: $T = 1$, $\sigma = 0.4$ and $S_0 = K = 100$. The exact value of this case is 15.85193755.

5.5.1 Weak error plots

In this section, we include the results of weak error rates for the call option for 2 scenarios, without/with Richardson extrapolation (level 1). We note that the weak errors plotted here correspond to relative errors. We note that in order to get accurate estimates of the bias, we needed to kill the laguerre quadrature error by increasing β (β : the number of quadrature points used for Laguerre to get $h(\mathbf{z}_{-1})$). For illustration, we show two cases $\beta = 10$ and $\beta = 32$. We mention that from our numerical experiences that the bias did not change as we increase β greater than 32 points.

Focusing on the results produced by setting $\beta = 32$ (which gives the right behavior to be observed for the bias), we can see from figure 10 that we get a weak error of order Δt for the case without Richardson extrapolation. From figure 11, we observe an improvement in the rate and the constant when using level 1 of Richardson extrapolation, approximately of order Δt^2 . For all the plots below, the upper and lower bounds are 95% confidence interval.

$\beta = 10$

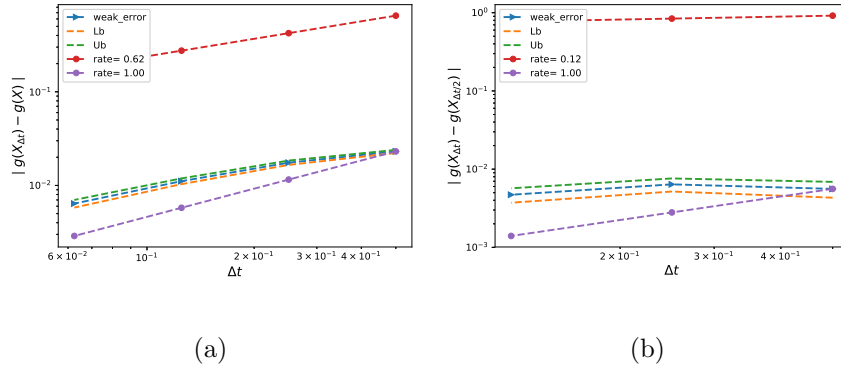
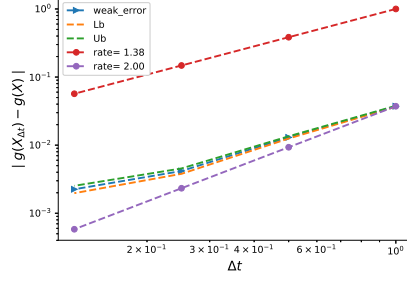
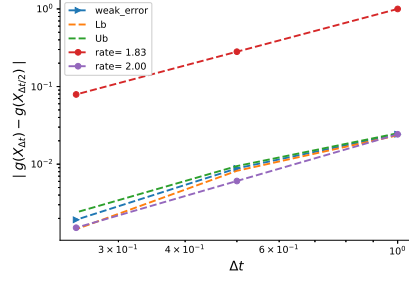


Figure 8: The rate of convergence of the weak error for the call option, without Richardson extrapolation, using MC with $M = 10^5$: a) $|E[g(X_{\Delta t})] - g(X)|$ b) $|E[g(X_{\Delta t}) - g(X_{\Delta t/2})]|$



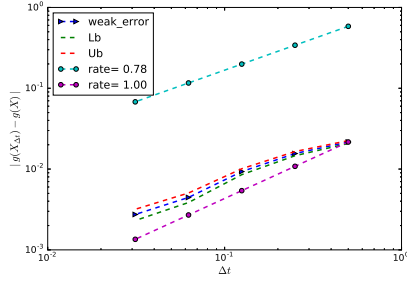
(a)



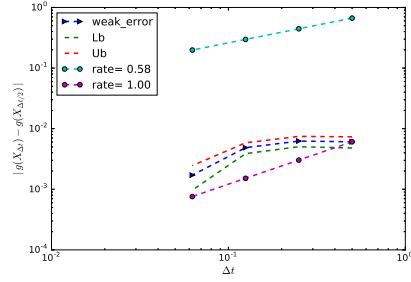
(b)

Figure 9: The rate of convergence of the weak error for the call option with Richardson extrapolation, using MC with $M = 10^6$: a) $|E[2g(X_{\Delta t/2}) - g(X_{\Delta t})] - g(X)|$ b) $|E[3g(X_{\Delta t/2}) - g(X_{\Delta t}) - 2g(X_{\Delta t/4})]|$

$\beta = 32$



(a)



(b)

Figure 10: The rate of convergence of the weak error for the call option, without Richardson extrapolation, using MC with $M = 10^5$: a) $|E[g(X_{\Delta t})] - g(X)|$ b) $|E[g(X_{\Delta t}) - g(X_{\Delta t/2})]|$

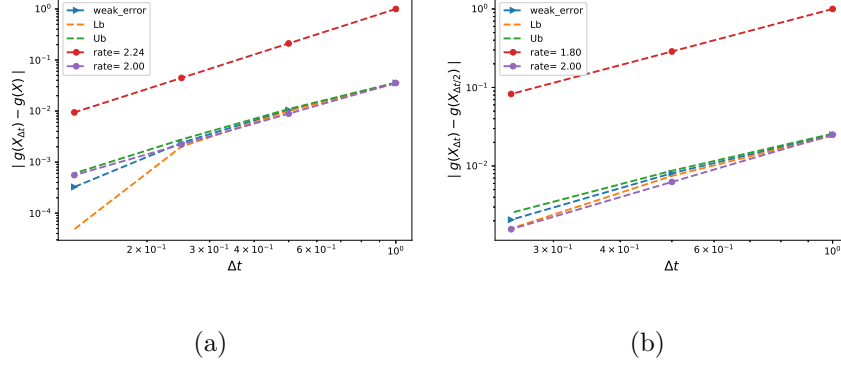


Figure 11: The rate of convergence of the weak error for the call option with Richardson extrapolation (level 1), using MC with $M = 5.10^6$: a) $|\mathbb{E}[2g(X_{\Delta t/2}) - g(X_{\Delta t})] - g(X)|$ b) $|\mathbb{E}[3g(X_{\Delta t/2}) - g(X_{\Delta t}) - 2g(X_{\Delta t/4})]|$

5.5.2 Comparing relative errors

Without Richardson extrapolation

In this Section, we report the results for the Call option, using the different Methods: MISC, MC + root finding and MC, without Richardson extrapolation. We mention that for MISC we used a very small tolerance for the Newton solver, when solving the Kink point problem ($TOL_{\text{Newton}} = 10^{-10}$), we also used $\beta = 32$ (number of Laguerre quadrature points). We start by reporting the observed approximated values using different methods (See table 11). The biased values for MC method were computed using the values of Bias, reported in table 12. In table 13, we report the behavior of quadrature error with respect to MISC tolerance. We precise that the quadrature error is computed by subtracting the MISC approximated value from the biased MC value. We report in red the values where MISC becomes stable (see also figure 12). Those values were used to compute the needed number of samples for MC (with and without root finding), to achieve similar magnitude for statistical error. Later, in table 14, we report the total relative error for all methods (Quadrature error + Bias for MISC and Statistical error + Bias for MC). We also report in table 15, the computational time needed for all different methods. We finally provide in figure 13, the complexity rates for the different involved methods.

Method \ Steps	2	4	8	16
MISC ($Tol = 5.10^{-1}, \beta = 32$)	16.184	16.070	15.998	15.930
MISC ($Tol = 10^{-1}, \beta = 32$)	16.184	16.070	15.996	15.928
MISC ($Tol = 5.10^{-2}, \beta = 32$)	16.184	16.070	15.996	15.928
MISC ($Tol = 10^{-2}, \beta = 32$)	16.184	16.103	15.996	15.928
MISC ($Tol = 10^{-3}, \beta = 32$)	16.184	16.103	15.996	—
MC method ($M = 10^5$)	16.194	16.099	15.999	15.923

Table 11: Call option price of the different methods for different number of time steps, without Richardson extrapolation.

Method \ Steps	2	4	8	16
MC Bias ($M = 10^5$)	0.0216 (0.3424)	0.0156 (0.2473)	0.0093 (0.1474)	0.0045 (0.0713)
MC Statistical error ($M = 10^5$)	4.4e-04 (7.5e-03)	4.7e-04 (7.5e-03)	4.0e-04 (6.3e-03)	3.1e-04 (4.9e-03)

Table 12: Bias and Statistical errors of MC for computing Call option price for different number of time steps, without Richardson extrapolation. The numbers between parentheses are the corresponding absolute errors.

Method \ Steps	2	4	8	16
MISC ($Tol = 5.10^{-1}$)	0.0007 (0.0103)	0.0018 (0.0290)	6.3e-05 (0.0010)	0.0004 (0.0070)
MISC ($Tol = 10^{-1}$)	0.0007 (0.0103)	0.0018 (0.0290)	0.0002 (0.0030)	0.0001 (0.0020)
MISC ($Tol = 5.10^{-2}$)	0.0007 (0.0103)	0.0018 (0.0290)	0.0002 (0.0030)	0.0001 (0.0020)
MISC ($Tol = 10^{-2}$)	0.0007 (0.0103)	0.0003 (0.0040)	0.0002 (0.0030)	0.0001 (0.0020)
MISC ($Tol = 10^{-3}$)	0.0007 (0.0103)	0.0003 (0.0040)	0.0002 (0.0030)	— (—)

Table 13: Quadrature error of MISC to compute Call option price of the different tolerances for different number of time steps, without Richardson extrapolation. The numbers between parentheses are the corresponding absolute errors.

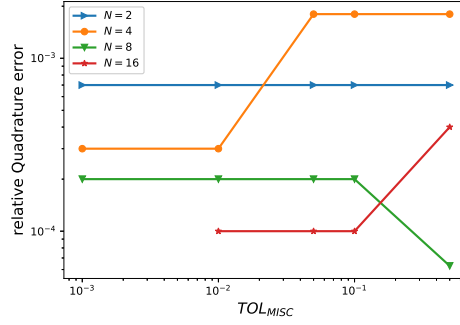


Figure 12: Relative quadrature error of MISC to compute Call option price of the different tolerances for different number of time steps, without Richardson extrapolation.

Method \ Steps	2	4	8	16
MISC ($Tol = 5.10^{-1}$)	0.0223	0.0174	0.0094	0.0049
MISC ($Tol = 10^{-1}$)	0.0223	0.0174	0.0095	0.0046
MISC ($Tol = 5.10^{-2}$)	0.0223	0.0174	0.0095	0.0046
MISC ($Tol = 10^{-2}$)	0.0223	0.0159	0.0095	0.0046
MISC ($Tol = 10^{-3}$)	0.0223	0.0159	0.0095	
MC +root finding	0.0223	0.0159	0.0095	0.0046
MC	0.0223	0.0159	0.0095	0.0046

Table 14: Total error of MISC and MC to compute Call option price of the different tolerances for different number of time steps, without Richardson extrapolation. The numbers between parentheses are the corresponding absolute errors.

Method \ Steps	2	4	8	16
MISC ($Tol = 5.10^{-1}$)	0.3	3	17	473
MISC ($Tol = 10^{-1}$)	0.3	3	58	656
MISC ($Tol = 5.10^{-2}$)	0.3	3	73	731
MISC ($Tol = 10^{-2}$)	0.3	6	108	1972
MISC ($Tol = 10^{-3}$)	0.3	28	264	—
MC method +root finding	1328	8140	21400	70200
MC method	1450	9990	32790	158108
Ratio of (MC+root finding)/(MISC)	$4.4e + 03$	$1.4e + 03$	369	107
Ratio of (MC)/(MISC)	$4.8e + 03$	1665	565	241

Table 15: Comparison of the computational time of MC and MISC, used to compute Call option price for different number of time steps, without Richardson extrapolation

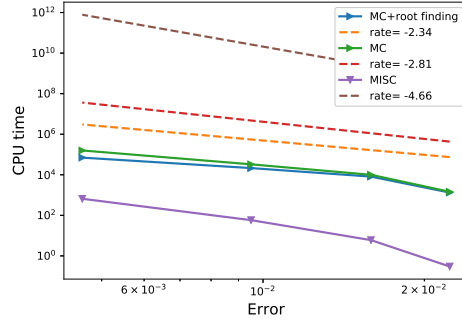


Figure 13: Complexity plot for MC and MISC for the case without Richardson extrapolation.

With Richardson extrapolation (level 1)

In this Section, we report the results for the Call option, using the different Methods: MISC, MC + root finding and MC, with Richardson extrapolation . We mention that for MISC we used a very

small tolerance for the Newton solver, when solving the Kink point problem ($TOL_{\text{Newton}} = 10^{-10}$), we also used $\beta = 32$ (number of Laguerre quadrature points). We start by reporting the observed approximated values using different methods (See table 16. The biased values for MC method were computed using the values of Bias, reported in table 17. In table 18, we report the behavior of quadrature error with respect to MISC tolerance. We precise that the quadrature error is computed by subtracting the MISC approximated value from the biased MC value. We report in red the values where MISC becomes stable (see also figure 14). Those values were used to compute the needed number of samples for MC (with and without root finding), to achieve similar magnitude for statistical error. Later, in table 19, we report the total relative error for all methods (Quadrature error + Bias for MISC and Statistical error + Bias for MC). We also report in table 20, the computational time needed for all different methods. We finally provide in figure 15, the comparison between the two versions of MISC (without/with Richardson extrapolation).

Method \Steps	1 – 2	2 – 4	4 – 8	8 – 16
MISC ($Tol = 5.10^{-1}$)	16.4108	16.0254	15.8912	15.8621
MISC ($Tol = 10^{-1}$)	16.4108	16.0254	15.8883	15.8603
MISC ($Tol = 5.10^{-2}$)	16.4108	16.0218	15.8885	15.8600
MISC ($Tol = 10^{-2}$)	16.4108	16.0218	15.8888	15.8595
MISC ($Tol = 10^{-3}$)	16.4108	16.0207	15.8885	–
MC method ($M = 5.10^6$)	16.4147	16.0184	15.8900	15.8567

Table 16: Call option price of the different methods for different number of time steps, with Richardson extrapolation (level 1).

Method \Steps	1 – 2	2 – 4	4 – 8	8 – 16
MC Bias ($M = 5.10^6$)	0.0355 (0.5627)	0.0105 (0.1664)	0.0024 (0.0380)	0.0003 (0.0048)
MC Statistical error ($M = 5.10^6$)	2.8e – 04 (4.4e–03)	2.4e – 04 (3.8e–03)	1.9e – 04 (3.0e–03)	1.4e – 04 (2.2e–03)

Table 17: Bias and Statistical errors of MC for computing Call option price for different number of time steps, with Richardson extrapolation (level 1). The numbers between parentheses are the corresponding absolute errors.

Method \ Steps	1 – 2	2 – 4	4 – 8	8 – 16
MISC ($Tol = 5.10^{-1}$)	2.5e – 04 (0.0039)	4.4e – 04 (0.0070)	7.6e – 05 (0.0012)	3.4e – 04 (0.0054)
MISC ($Tol = 10^{-1}$)	2.5e – 04 (0.0039)	4.4e – 04 (0.0070)	1.1e – 04 (0.0017)	2.3e – 04 (0.0036)
MISC ($Tol = 5.10^{-2}$)	2.5e – 04 (0.0039)	2.1e – 04 (0.0034)	9.5e – 05 (0.0015)	2.1e – 04 (0.0033)
MISC ($Tol = 10^{-2}$)	2.5e – 04 (0.0039)	2.1e – 04 (0.0034)	7.6e – 05 (0.0012)	1.7e – 04 (0.0028)
MISC ($Tol = 10^{-3}$)	2.5e – 04 (0.0039)	1.5e – 04 (0.0023)	9.5e – 05 (0.0015)	()

Table 18: Quadrature error of MISC to compute Call option price of the different tolerances for different number of time steps, with Richardson extrapolation (level 1). The numbers between parentheses are the corresponding absolute errors.

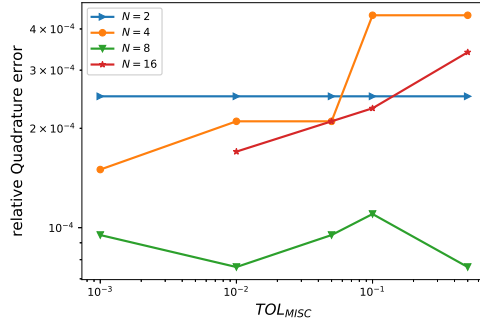


Figure 14: Relative quadrature error of MISC to compute Call option price of the different tolerances for different number of time steps, with Richardson extrapolation.

Method \ Steps	1 – 2	2 – 4	4 – 8	8 – 16
MISC ($Tol = 5.10^{-1}$)	0.0358	0.0109	0.0025	0.0006
MISC ($Tol = 10^{-1}$)	0.0358	0.0109	0.0025	0.0005
MISC ($Tol = 5.10^{-2}$)	0.0358	0.0107	0.0025	0.0005
MISC ($Tol = 10^{-2}$)	0.0358	0.0107	0.0025	0.0005
MISC ($Tol = 10^{-3}$)	0.0358	0.0107	0.0025	

Table 19: Total error of MISC to compute Call option price of the different tolerances for different number of time steps, with Richardson extrapolation (level 1). The numbers between parentheses are the corresponding absolute errors.

Method \ Steps	1 – 2	2 – 4	4 – 8	8 – 16
MISC ($Tol = 5 \cdot 10^{-1}$)	0.3	4	56	713
MISC ($Tol = 10^{-1}$)	0.3	4	107	1126
MISC ($Tol = 5 \cdot 10^{-2}$)	0.3	9	135	1253
MISC ($Tol = 10^{-2}$)	0.3	9	186	3540
MISC ($Tol = 10^{-3}$)	0.3	63	836	

Table 20: Comparison of the computational time of MISC, used to compute Call option price for different number of time steps, with Richardson extrapolation (level 1)

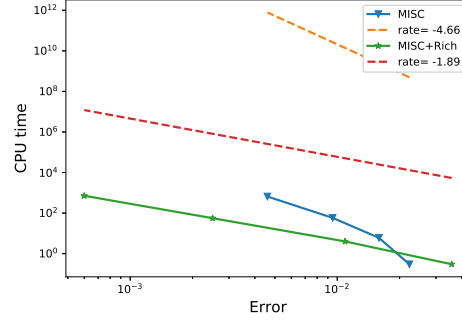


Figure 15: Complexity plot for MISC without and with Richardson extrapolation, for the Call option.

5.6 Result for the 2-dimensional Basket call option

5.6.1 Weak error plots

We consider the case of 2-dimensional Basket call option, with parameters: $S^{(1,2)} = 100$, $K = 100$, $\sigma^{(1,2)} = 0.4$, $\rho = 0.3$, $r = 0$, $T = 1$. The MC value of this case (with large number of samples) is 12.900784 with a statistical error equal to 0.001033 (Provided by Premia).

In this section, we include the results of weak error rates for 2 scenarios, without/with Richardson extrapolation (level 1). We note that the weak errors plotted here correspond to relative errors.

We can see from figure 16 that we get a weak error of order Δt for the case without Richardson extrapolation.

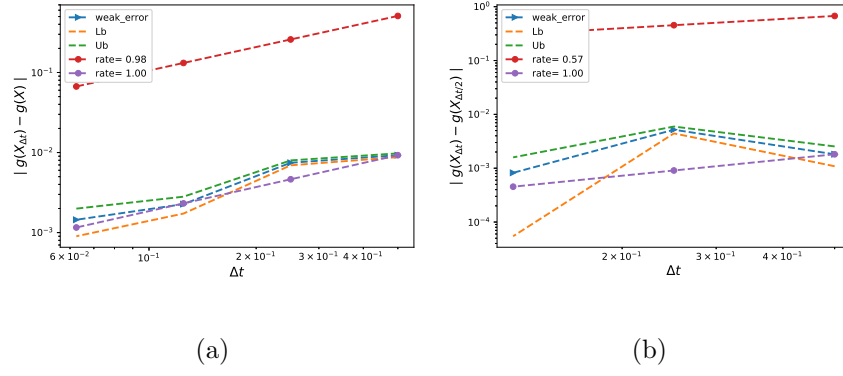


Figure 16: The rate of convergence of the weak error for the Basket (2-dimensional) call option, without Richardson extrapolation, using MC with $M = 4.10^7$: a) $|E[g(X_{\Delta t})] - g(X)|$ b) $|E[g(X_{\Delta t/2}) - g(X_{\Delta t/2})]|$

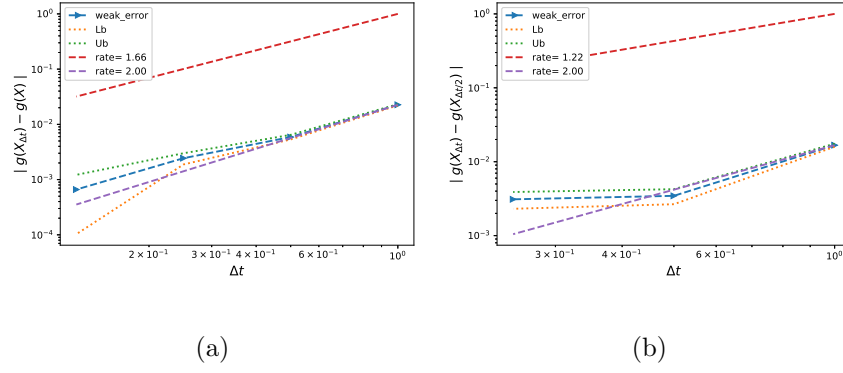


Figure 17: The rate of convergence of the weak error for the Basket (2-dimensional) call option with Richardson extrapolation (level 1), using MC with $M = 4.10^7$: a) $|E[2g(X_{\Delta t/2}) - g(X_{\Delta t})] - g(X)|$ b) $|E[3g(X_{\Delta t/2}) - g(X_{\Delta t}) - 2g(X_{\Delta t/4})]|$

5.6.2 Comparing relative errors

Without Richardson extrapolation

Method \Steps	2	4	8	16
MISC ($Tol = 5.10^{-1}, \beta = 16$)	13.0009	12.8577	12.8854	12.9000
MISC ($Tol = 10^{-1}, \beta = 16$)	13.0009	12.9912	12.9556	12.9231
MISC ($Tol = 5.10^{-2}, \beta = 16$)	13.0009	13.0049	12.9550	—
MISC ($Tol = 10^{-2}, \beta = 16$)	13.0548	13.0046	12.9550	—
MISC ($Tol = 10^{-3}, \beta = 16$)	13.0548	13.0046	—	—
MISC ($Tol = 10^{-4}, \beta = 16$)	13.0545	13.0047	—	—
MISC ($Tol = 10^{-5}, \beta = 16$)	13.0545	—	—	—
MC method ($M = 4.10^7$)	13.0203	12.9969	12.9301	12.9194

Table 21: Basket (2-dimensional) Call option price of the different methods for different number of time steps, without Richardson extrapolation.

Method \Steps	2	4	8	16
MC Bias ($M = 4.10^7$)	0.0093 (0.1195)	0.0075 (0.0968)	0.0023 (0.0297)	0.0014 (0.0181)
MC Statistical error ($M = 4.10^7$)	2.5e-04 (3.2e-03)	2.7e-04 (3.5e-03)	2.8e-04 (3.6e-03)	2.8e-04 (3.6e-03)

Table 22: Bias and Statistical errors of MC for computing Basket (2-dimensional) Call option price for different number of time steps, without Richardson extrapolation. The numbers between parentheses are the corresponding absolute errors.

Method \Steps	2	4	8	16
MISC ($Tol = 5.10^{-1}$)	0.0015 (0.0194)	0.0108 (0.1392)	0.0035 (0.0447—)	0.0015 (0.0194)
MISC ($Tol = 10^{-1}$)	0.0015 (0.0194)	4.4e-04 (0.0057)	0.0020 (0.0255)	2.9e-04 (0.0037)
MISC ($Tol = 5.10^{-2}$)	0.0015 (0.0194)	6.2e-04 (0.0080)	0.0019 (0.0249)	— (—)
MISC ($Tol = 10^{-2}$)	0.0027 (0.0345)	6.0e-04 (0.0077)	0.0019 (0.0249)	— (—)
MISC ($Tol = 10^{-3}$)	0.0027 (0.0345)	6.0e-04 (0.0077)	— (—)	— (—)
MISC ($Tol = 10^{-4}$)	0.0027 (0.0342)	6.0e-04 (0.0078)	— (—)	— (—)
MISC ($Tol = 10^{-5}$)	0.0027 (0.0342)	— (—)	— (—)	— (—)

Table 23: Quadrature error of MISC to compute Basket (2-dimensional) Call option price of the different tolerances for different number of time steps, without Richardson extrapolation. The numbers between parentheses are the corresponding absolute errors.

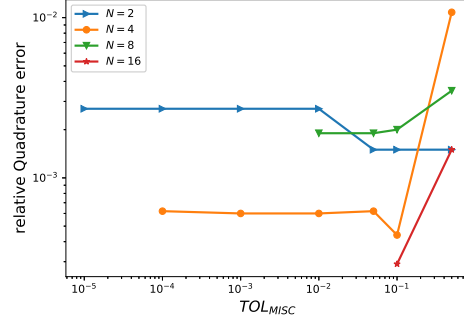


Figure 18: Relative quadrature error of MISC to compute Basket (2-dimensional) Call option price of the different tolerances for different number of time steps, without Richardson extrapolation.

Method \ Steps	2	4	8	16
MISC ($Tol = 5 \cdot 10^{-1}$)	0.0108	0.0183	0.0058	0.0029
MISC ($Tol = 10^{-1}$)	0.0108	0.0079	0.0043	0.0017
MISC ($Tol = 5 \cdot 10^{-2}$)	0.0108	0.0081	0.0042	—
MISC ($Tol = 10^{-2}$)	0.0120	0.0081	0.0042	—
MISC ($Tol = 10^{-3}$)	0.0120	0.0081	—	—
MISC ($Tol = 10^{-4}$)	0.0120	0.0081	—	—
MISC ($Tol = 10^{-5}$)	0.0120	—	—	—
MC +root finding	0.0120	0.0081	0.0042	0.0029
MC	0.0119	0.0081	0.0042	0.0029

Table 24: Total error of MISC and MC to compute Basket (2-dimensional) Call option price of the different tolerances for different number of time steps, without Richardson extrapolation. The numbers between parentheses are the corresponding absolute errors.

Method \ Steps	2	4	8	16
MISC ($Tol = 5.10^{-1}$)	3	15	197	1048
MISC ($Tol = 10^{-1}$)	3	34	217	7324
MISC ($Tol = 5.10^{-2}$)	3	44	917	—
MISC ($Tol = 10^{-2}$)	4	98	1825	—
MISC ($Tol = 10^{-3}$)	4	245	—	—
MISC ($Tol = 10^{-4}$)	23	1035	—	—
MISC ($Tol = 10^{-5}$)	58	—	—	—
MC method +root finding	557	13564	1218	1749
MC method	164	3518	451	1112
Ratio of (MC+root finding)/(MISC)	139	308	5.6	1.7
Ratio of (MC)/(MISC)	41	80	2.1	1.1

Table 25: Comparison of the computational time of MC and MISC, used to compute Basket (2-dimensional) Call option price for different number of time steps, without Richardson extrapolation

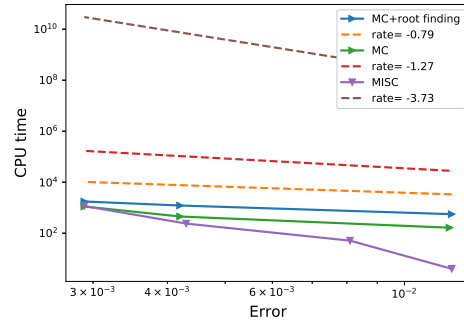


Figure 19: Complexity plot for MC and MISC for the case without Richardson extrapolation.

With Richardson extrapolation (level 1)

Method \ Steps	1 – 2	2 – 4	4 – 8
MISC ($Tol = 5.10^{-1}, \beta = 16$)	13.0821	12.7353	12.8138
MISC ($Tol = 10^{-1}, \beta = 16$)	13.1898	12.8791	12.9055
MISC ($Tol = 5.10^{-2}, \beta = 16$)	13.1898	12.9151	—
MISC ($Tol = 10^{-2}, \beta = 16$)	13.1898	12.9567	—
MISC ($Tol = 10^{-3}, \beta = 16$)	13.1898	12.9558	—
MISC ($Tol = 10^{-4}, \beta = 16$)	13.1893	—	—
MC method ($M = 4.10^7$)	13.1927	12.9768	12.9322

Table 26: Basket 2-dimensional Call option price of the different methods for different number of time steps, with Richardson extrapolation (level 1).

Method \ Steps	1 – 2	2 – 4	4 – 8	8 – 16
MC Bias ($M = 4.10^7$)	0.0226 (0.2919)	0.0059 (0.0760)	0.0024 (0.0314)	0.0007 (0.0085)
MC Statistical error ($M = 4.10^7$)	2.9e – 04 (3.7e–03)	2.9e – 04 (3.7e–03)	2.9e – 04 (3.7e–03)	2.8e – 04 (3.6e–03)

Table 27: Bias and Statistical errors of MC for computing Basket (2-dimensional) Call option price for different number of time steps, with Richardson extrapolation (level 1). The numbers between parentheses are the corresponding absolute errors.

Method \ Steps	1 – 2	2 – 4	4 – 8
MISC ($Tol = 5.10^{-1}$)	0.0086 (0.1106)	0.0187 (0.2415)	0.0092 (0.1184)
MISC ($Tol = 10^{-1}$)	0.0002 (0.0029)	0.0076 (0.0977)	0.0021 (0.0267)
MISC ($Tol = 5.10^{-2}$)	0.0002 (0.0029)	0.0048 (0.0617)	— (—)
MISC ($Tol = 10^{-2}$)	0.0002 (0.0029)	0.0016 (0.0201)	— (—)
MISC ($Tol = 10^{-3}$)	0.0002 (0.0029)	0.0016 (0.0210)	— (—)
MISC ($Tol = 10^{-4}$)	0.0002 (0.0029)	— (—)	— (—)

Table 28: Quadrature error of MISC to compute Basket (2-dimensional) call option price of the different tolerances for different number of time steps, with Richardson extrapolation. The numbers between parentheses are the corresponding absolute errors.

Method \ Steps	1 – 2	2 – 4	4 – 8
MISC ($Tol = 5.10^{-1}$)	0.0312	0.0246	0.0116
MISC ($Tol = 10^{-1}$)	0.0228	0.0135	0.0045
MISC ($Tol = 5.10^{-2}$)	0.0228	0.0107	—
MISC ($Tol = 10^{-2}$)	0.0228	0.0075	—
MISC ($Tol = 10^{-3}$)	0.0228	0.0075	—
MISC ($Tol = 10^{-4}$)	0.0228	—	—
MC +root finding	—	—	—
MC	—	—	—

Table 29: Total relative error of MISC and MC to compute Basket (2-dimensional) call option price of the different tolerances for different number of time steps, with Richardson extrapolation. The numbers between parentheses are the corresponding absolute errors.

Method \ Steps	1 – 2	2 – 4	4 – 8
MISC ($Tol = 5.10^{-1}$)	5	39	396
MISC ($Tol = 10^{-1}$)	8	70	1379
MISC ($Tol = 5.10^{-2}$)	8	76	–
MISC ($Tol = 10^{-2}$)	8	262	–
MISC ($Tol = 10^{-3}$)	8	339	–
MISC ($Tol = 10^{-4}$)	55	–	–

Table 30: Comparison of the computational time of MISC, used to compute Basket 2-dimensional Call option price for different number of time steps, with Richardson extrapolation (level 1)

5.7 The basket option with the smoothing trick as in [2]

The third experiment that we consider is the pricing of a European basket call option in a Black-Scholes model. The basket is composed of d assets ($d = 3, 8, 25$) and we use the same trick of smoothing the integrand that was proposed in [2]. In this case, the dimension of the parameter space $N = d - 1$. The interpolation over the parameter space is based on the tensorized Lagrangian interpolation technique with Gaussian points. The aim of this section is to check the performance of MISC without time stepping. The main goal is to extend this case to the time stepping framework in the next section 5.2

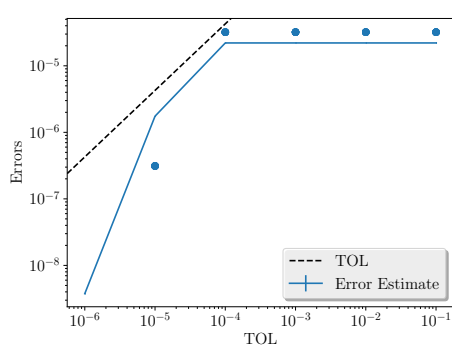
5.7.1 Results using MISC

In table 31, we summarize the observed complexity rates for different tested settings for the basket example. From this table, we can check that even with the 25 dimensional case, the complexity rate in terms of the elapsed time is at least order 1, which is better than MC, which is 2. Detailed plots for each case are given by figures (20, 21) for $d = 3$, figures (22, 23) for $d = 8$ and figures (24, 25) for $d = 25$. Mainly, from the plots, we checked that we achieve the prescribed tolerance using MISC, the convergence rates of mixed differences which is a basic assumption for using MISC (we observe exponential decay of error rates wrt to the number of quadrature points) and finally the complexity rates. In the next Section, we try to extend these results to the time stepping framework.

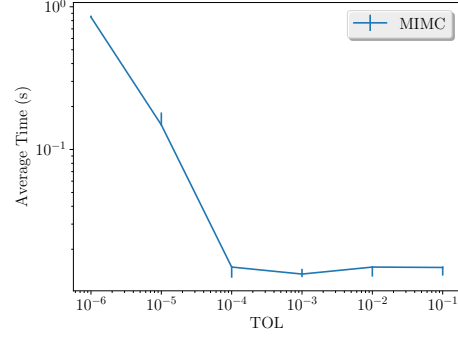
# assets \	3	8	25
rate	$-1/3$	$-9/20$	$-16/25$

Table 31: Complexity rates of the different experiments for the basket option using BS model

Case of 3-dimensional Basket

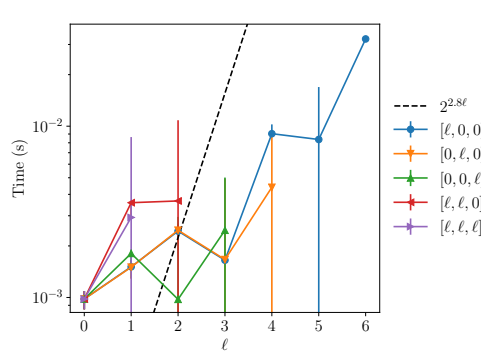


(a) Error estimate

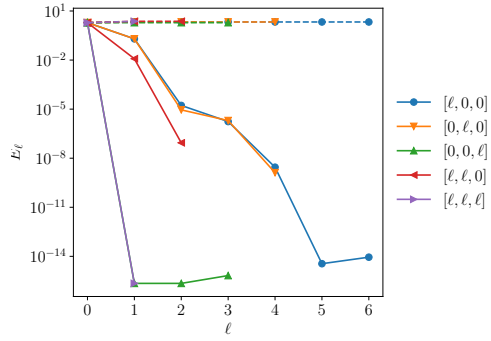


(b) Average running time as a function of TOL

Figure 20: Convergence and complexity results for the 3-dimensional basket option using BS model.



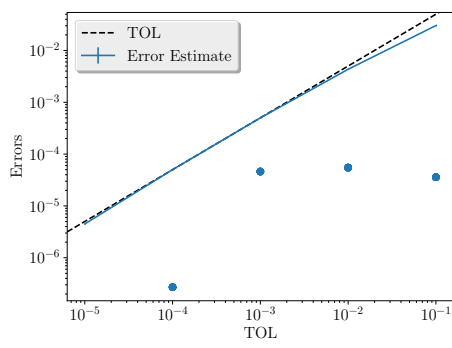
(a) Average Computational time per level.



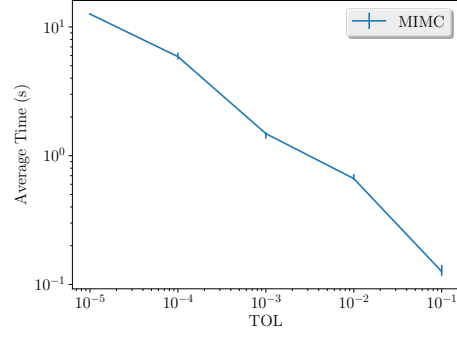
(b) The convergence rate of mixed differences per level.

Figure 21: Convergence and work rates for discretization levels for the 3-dimensional basket option using BS model.

Case of 8-dimensional Basket

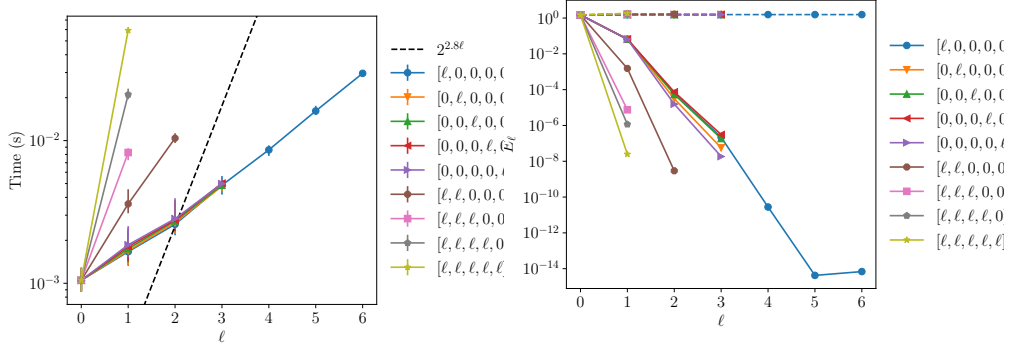


(a) Error estimate



(b) Average running time as a function of TOL

Figure 22: Convergence and complexity results for the 8-dimensional basket option using BS model.



(a) Average Computational time per level. (b) The convergence rate of mixed differences per level.

Figure 23: Convergence and work rates for discretization levels for the 8-dimensional basket option using BS model.

Case of 25-dimensional Basket

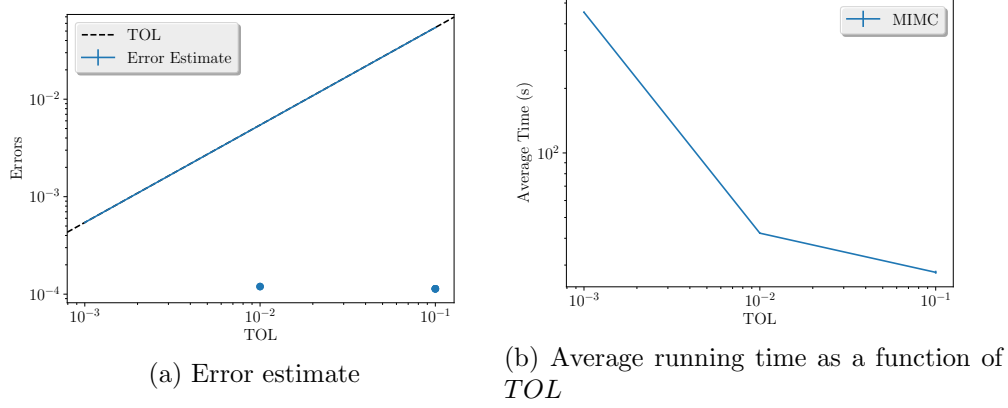


Figure 24: Convergence and complexity results for the 25-dimensional basket option using BS model.

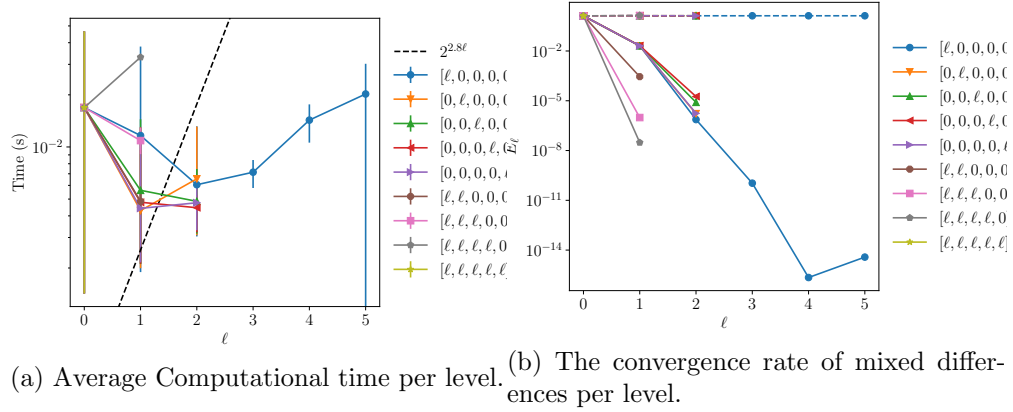


Figure 25: Convergence and work rates for discretization levels for the 25-dimensional basket option using BS model.

References Cited

- [1] Peter A Acworth, Mark Broadie, and Paul Glasserman. A comparison of some monte carlo and quasi monte carlo techniques for option pricing. In *Monte Carlo and Quasi-Monte Carlo Methods 1996*, pages 1–18. Springer, 1998.
- [2] CHRISTIAN BAYER, MARKUS SIEBENMORGEN, and RAUL TEMPONE. Smoothing the payoff for efficient computation of basket option pricing.
- [3] Hans-Joachim Bungartz and Michael Griebel. Sparse grids. *Acta numerica*, 13:147–269, 2004.
- [4] Russel E Caflisch, William J Morokoff, and Art B Owen. *Valuation of mortgage backed securities using Brownian bridges to reduce effective dimension*. 1997.

- [5] Thomas Gerstner. Sparse grid quadrature methods for computational finance.
- [6] Thomas Gerstner and Markus Holtz. Valuation of performance-dependent options. *Applied Mathematical Finance*, 15(1):1–20, 2008.
- [7] Paul Glasserman. *Monte Carlo methods in financial engineering*. Springer, New York, 2004.
- [8] Michael Griebel, Frances Kuo, and Ian Sloan. The smoothing effect of integration in $\hat{\{\}}$ and the anova decomposition. *Mathematics of Computation*, 82(281):383–400, 2013.
- [9] Michael Griebel, Frances Kuo, and Ian Sloan. Note on the smoothing effect of integration in $\hat{\{\}}$ and the anova decomposition. *Mathematics of Computation*, 86(306):1847–1854, 2017.
- [10] Andreas Griewank, Frances Y Kuo, Hernan Leövey, and Ian H Sloan. High dimensional integration of kinks and jumps—smoothing by preintegration. *arXiv preprint arXiv:1712.00920*, 2017.
- [11] Abdul-Lateef Haji-Ali, Fabio Nobile, Lorenzo Tamellini, and Raul Tempone. Multi-index stochastic collocation for random pdes. *Computer Methods in Applied Mechanics and Engineering*, 306:95–122, 2016.
- [12] Gerhard Larcher, Gunther Leobacher, and Klaus Scheicher. On the tractability of the brownian bridge algorithm. *Journal of Complexity*, 19(4):511–528, 2003.
- [13] William J Morokoff. Generating quasi-random paths for stochastic processes. *Siam Review*, 40(4):765–788, 1998.
- [14] Bradley Moskowitz and Russel E Caflisch. Smoothness and dimension reduction in quasi-monte carlo methods. *Mathematical and Computer Modelling*, 23(8):37–54, 1996.
- [15] Denis Talay and Luciano Tubaro. Expansion of the global error for numerical schemes solving stochastic differential equations. *Stochastic analysis and applications*, 8(4):483–509, 1990.
- [16] Ye Xiao and Xiaoqun Wang. Conditional quasi-monte carlo methods and dimension reduction for option pricing and hedging with discontinuous functions. *Journal of Computational and Applied Mathematics*, 343:289–308, 2018.